Study of LINER sources with broad H α emission

G. Younes, D. Porquet, B. Sabra, J. Reeves, N. Grosso

A&A 539, A104 (2012)
DOI: 10.1051/0004-6361/201118299

Astronomy & Astrophysics

Study of LINER sources with broad Hα emission

Spectral energy distribution and multiwavelength correlations

G. Younes[1], D. Porquet[1], B. Sabra[2], J. N. Reeves[3,4], and N. Grosso[1]

[1] Observatoire Astronomique de Strasbourg, Université de Strasbourg, CNRS, UMR7550, 11 rue de l'Université, 67000 Strasbourg, France
e-mail: georges.younes@astro.unistra.fr
[2] Department of Physics & Astronomy, Notre Dame University-Louaize, PO Box 72, Zouk Mikael, Lebanon
[3] Astrophysics Group, School of Physical & Geographical Sciences, Keele University, Keele, Staffordshire ST5 5BG, UK
[4] Department of Physics, University of Maryland Baltimore County, Baltimore, MD 21250, USA

Received 19 October 2011 / Accepted 25 January 2012

ABSTRACT

Context. The geometry and physical properties of the accretion mode, and the radiative processes occurring in AGN-powered low ionization nuclear emission-line regions (LINERs) remain a riddle. Both a standard thin accretion disk and an inner-hot radiatively-inefficient accretion flow (RIAF) have been invoked. Models depending on only a jet have also been invoked to explain the broad-band spectral energy distribution (SED) of LINERs.
Aims. We attempt to infer the accretion mechanism and radiative processes giving rise to the SEDs of a well-defined optically-selected sample of LINERs showing a definite detection of broad Hα emission (LINER 1s).
Methods. We construct SEDs for six LINER 1s with *simultaneous UV and X-ray fluxes*, and we looked for multiwavelength, radio to X-ray and UV to X-ray, correlations.
Results. At a given X-ray luminosity, the average SED of the six LINER 1s in our sample: (1) resembles the SED of radio-loud quasars in the radio band, $\langle \log\ R_{\rm X} \rangle \approx -2.7$, (2) exhibits a weak UV bump, $\langle \alpha_{\rm ox} \rangle \approx -1.17 \pm 0.02$ with a dispersion $\sigma = 0.01$, and (3) displays a X-ray spectrum similar to radio-quiet quasars. The bolometric luminosities inferred from the SEDs of these LINER 1s are extremely faint, at least two orders of magnitude lower than AGN. The X-ray bolometric correction, $\kappa_{2-10\ \rm keV}$, of our sample is lower than in the case of AGN, with a mean value of 16. We find a strong anticorrelation between the radio loudness parameter, $R_{\rm X}$, and the Eddington ratio for our sample, confirming previous results. Moreover, we find a positive correlation between the radio luminosity and the X-ray luminosity which places AGN-powered LINERs, on a radio-power scale, right between low luminosity Seyferts and low luminosity radio galaxies. We complement our $\alpha_{\rm ox}$ list with values derived on a well defined sample of UV-variable LINERs, and establish a strong positive correlation between $\alpha_{\rm ox}$ (considering negative values) and the Eddington ratio, in contrast to the correlation found for luminous AGN. Lastly, we tested two different fundamental planes existing in the literature on our sample, in an attempt to put constraints on the debated origin of the X-ray emission, "RIAF versus jet". The results came contradictory with one pointing toward a RIAF-dominated X-ray emission process and the other pointing toward a jet domination.

Key words. accretion, accretion disks – galaxies: active – galaxies: nuclei – X-rays: galaxies

1. Introduction

Our nearby universe is mostly populated by galaxies showing low nuclear activity (see Ho 2008, and references therein). The most common component of these nearby low luminosity active galactic nuclei (LLAGN[1]) is low ionization nuclear emission-line regions (LINERs; Heckman 1980). These LINERs are characterized by optical spectra dominated by neutral or singly ionized species (e.g., O I), hence, non-AGN continua could in principle give rise to their optical spectra. Indeed, since the time of their establishment as a class, the excitation mechanism of LINERs has been a matter of an ongoing debate and could be explained in terms of: shock heated gas (Dopita & Sutherland 1995), starburst activity (Terlevich & Melnick 1985; Alonso-Herrero et al. 2000), or a LLAGN. Many multiwavelength studies were attributed to this subject, looking for a radio, sometimes variable, core (Nagar et al. 2005) or a variable UV core (Maoz et al. 2005). Nevertheless, the most used tool to search for an active nucleus in a LINER is to look for a hard 2–10 keV unresolved core that could not be due to diffuse emission from shock heated gas or from unusually hot stars (Terashima et al. 2000; Ho et al. 2001; Dudik et al. 2005; Flohic et al. 2006; González-Martín et al. 2006, 2009; Zhang et al. 2009). How do LINERs harboring a low luminosity active nucleus compare to luminous Seyfert galaxies and quasars?

Active galactic nuclei (AGN), including Seyfert galaxies and quasars, emit a broad band spectral energy distribution (SED) from radio all the way up to X-rays, sometimes even gamma-rays. The most prominent feature in the SED of AGN is a broad UV excess, known as the "big blue bump" (e.g., Elvis et al. 1994). This UV excess, along with many other signatures characterizing AGN; e.g., the high bolometric luminosities ($L_{\rm bol} \geq 10^{44}$) and Eddington ratios ($L_{\rm bol}/L_{\rm Edd} \geq 10^{-2}$, where $L_{\rm Edd}$ represents the Eddington luminosity; Porquet et al. 2004; Vasudevan & Fabian 2009; Vasudevan et al. 2009; Grupe et al. 2010), the rapid X-ray variability on time-scales of hours to days (Turner et al. 1999), and the gravitationally redshifted Fe emission line profile (Nandra et al. 2007), are believed to be achieved

[1] Hereafter, the term LLAGN designate the definite existence of an AGN at a given galaxy center, but with an Eddington ratio $\leq 10^{-3}$.

through accretion onto a supermassive black hole (SMBH), in the form of a geometrically thin optically thick accretion disk (Shakura & Sunyaev 1973; Shields 1978; Malkan & Sargent 1982).

Contrary to classical AGN, where at least a somewhat universal accretion mode is thought to occur, the accretion physics and radiative processes taking place in LLAGN, including AGN-powered LINERs, have been a riddle so far. LINERs are extremely faint sources with X-ray luminosities almost never surpassing 10^{43} erg s^{-1} and Eddington ratios lower than $\sim 10^{-3}$, and explaining their faintness is a very challenging task.

The geometrically thin accretion disk, believed to power AGN, has been invoked as a LINER source of power as well. From an observational point of view, Maoz (2007), using high angular resolution multiwavelength observations of 13 UV-variable LINER sources, demonstrated that the luminosity ratios in different wavebands, mainly UV to X-ray and radio to UV, follow the same trend as luminous Seyfert galaxies. The authors did not find any sharp change in the SED of their sample compared to more luminous Seyfert and quasar nuclei, suggesting that a thin accretion disk may persist at low Eddington ratios. Pian et al. (2010) combined *Swift* XRT X-ray fluxes with simultaneous UV fluxes coming from the UVOT instrument and showed, similar to Maoz (2007), that the SED and the UV to X-ray flux ratios of their sample of 4 LINERs are consistent with those of more luminous sources, hence, implying that LINERs may have similar accretion and radiative processes at their center compared to luminous Seyfert nuclei.

On the other hand, the faintness of LINER sources compared to classical AGN has been attributed to a different accretion mechanism owing to some observational contrast between the two classes. In the X-ray domain, no broad nor narrow Fe Kα emission line at 6.4 keV have been detected in the spectra of the LINER sources with the highest signal to noise ratio (Ptak et al. 2004; Younes et al. 2011, hereafter Paper I), with only a few sources exhibiting short time-scale X-ray variability (Ptak et al. 1998; Awaki et al. 2001; Binder et al. 2009; Younes et al. 2010). Furthermore, early investigations of the multiwavelength properties of LLAGN, including LINERs, indicated that their SED might depart from the standard SED of classical AGN, especially in the UV band. Ho et al. (1996) reported the absence of the UV bump in the SED of the LINER source M 81, so did Nicholson et al. (1998) for the LINER nucleus of NGC 4594. The evidence for the faintness of the UV component in the SED of LINERs started to pile up with the study of bigger samples. Ho (1999; see also Eracleous et al. 2010) collected high spatial resolution multiwavelength fluxes for a sample of seven LLAGN. The author stated that the SED of the full sample looks markedly different than the SED of luminous AGN, noting that the UV emission is weaker, lacking the canonical UV bump. Moreover, Ho (1999) signalized that all of his LLAGN SEDs could be considered as radio-loud sources. These observational dissimilarities between LINERs/LLAGN and classical AGN may indicate the truncation/disappearance of the thin accretion disk at low luminosities, and therefore, a different accretion mechanism powering the emission in AGN-powered LINERs. Indeed, it has been suggested that when the mass accretion rate falls below a critical value $\dot{M}_{\rm crit}$, for which LINERs/LLAGN clearly belong to (Ho 2009), the density of the disk could become too low for radiative cooling to be effective. The trapped heat will expand the thin accretion disk into a pressure-supported thick disk with a very low radiative efficiency (see Quataert 2001; Yuan 2007; Narayan & McClintock 2008, for reviews). Such radiatively inefficient accretion flow (RIAF) models successfully explained the SED of a large number of LINER sources (Quataert et al. 1999; Gammie et al. 1999; Ptak et al. 2004; Nemmen et al. 2006; Wu et al. 2007; Yu et al. 2011).

The early RIAF solutions showed that the gravitational energy of the accretion flow could be lost, not only through convection, but also through outflowing winds and jets (e.g., Narayan & Yi 1994, 1995b; Blandford & Begelman 1999). Numerical and magnetohydrodynamic (MHD) simulations confirmed this finding and showed that RIAFs are associated with strong outflows (e.g., Igumenshchev & Abramowicz 2000; Hawley & Balbus 2002; Igumenshchev 2004), and even a component along the axis of the accretion flow in the form of a collimated relativistic jet (McKinney 2006). Observational evidence strengthened the idea of low accreting objects to produce outflows and relativistic jets since an important percentage of LINERs/LLAGN showed arcsecond or milliarcsecond jets (e.g., Nagar et al. 2001). Even the sources lacking a jet-like component on milliarcsecond scale were observed to harbor an unresolved radio core that have a high surface brightness temperature and a flat or slightly inverted radio spectrum, classic signatures of the presence of a relativistic jet (Blandford & Konigl 1979). Through synchrotron and synchrotron self-Compton processes, the jet could contribute to the broad-band emission of these low accreting sources, sometimes even dominating the accretion flow emission. Indeed, what is giving rise to the broad-band spectrum, especially the hard X-ray emission, is a highly debated subject, with some crediting completely the RIAF models, others leaning towards a jet origin (Falcke & Markoff 2000; Yuan et al. 2002a,b; Wu et al. 2007; Markoff et al. 2008).

The previous SED studies of LINERs/LLAGN, however, dealt with non-simultaneous UV and X-ray observations, sometimes separated by several years. LINERs, similar to AGN, show a high level of variability on years time-scales, mainly in the UV and X-ray bands (Paper I; Maoz et al. 2005; Pian et al. 2010). This variability factor if ignored could lead to inconsistencies in the LINER SEDs, strengthening or undermining the UV excess in these particular sources. Since the accretion physics rely heavily on the strength of the UV excess relative to X-rays, this important point should continuously be kept in mind.

Finally, there is an increasing number of evidence indicating that LINERs/LLAGN exist in a different spectral state compared to classical AGN, displaying a behavior similar to transient X-ray binaries (XRBs, Done 2002; Remillard & McClintock 2006; Done et al. 2007). In this context LINERs/LLAGN would be similar to XRBs during their low/hard state, showing very low bolometric luminosities (e.g., Paper I), and classical AGN would be analogous to high/soft state XRBs, with Eddington ratios $\geq$0.1 (e.g., Sobolewska et al. 2009). Recently, Sobolewska et al. (2011) predicted, by simulating the spectra of a sample of AGN based on the evolution pattern of the transient BH binary GRO J1655–40, that the UV-to-X-ray flux-ratio dependence on the Eddington ratio should change signs at $L_{\rm bol}/L_{\rm Edd} \approx 10^{-2}$. This change of sign, if observed, could represent another evidence supporting the idea of LINERs being in a different spectral state compared to classical AGN.

In this work, we revisit the SEDs of AGN-powered LINERs in an attempt to put constraints on the accretion mode and radiative processes of this class. To ensure the presence of an AGN at the center of our LINERs, only those showing a definite detection of a broad Hα emission where selected (Paper I; Ho et al. 1997b, LINER 1s hereafter). We briefly re-introduce our sample in Sect. 2, Sect. 3 represents the data compilation used to construct reliable SEDs with simultaneous UV and X-ray fluxes, and

gives the results of the different flux ratios. We give the properties of the different LINER 1 SEDs and of their mean, which represents to some extent the mean SED of all AGN-powered LINERs, in Sect. 4. We discuss our results in Sect. 5 in the context of accretion physics and radiative properties occurring in AGN-powered LINERs. Finally, we summarize our findings in Sect. 6. In the remainder of this paper, luminosities are calculated using the distances given in Table 1 of Paper I derived with a Hubble constant $H_0 = 75$ km s^{-1} Mpc^{-1}.

2. The sample

The LINER sample studied here has been introduced in a companion paper (Paper I). The sample comprises only the LINERs showing the definite detection of a broad Hα emission (LINER 1s, Ho et al. 1997b), and observed with either the *Chandra* and/or the *XMM-Newton* telescopes. This resulted in 13 LINER 1s. This class of LINER 1s ensures the definite existence of an AGN at the center of all of the selected galaxies and its responsibility for the excitation of the detected optical emission lines (Terashima et al. 2000). Moreover and according to the unification scheme of AGN, the central emission of LINER 1s should not be affected by the circumnuclear dust in the torus (if existing). The reader is referred to Paper I for more details on the general properties of the sample.

3. Results

3.1. SED construction with simultaneous UV and X-ray fluxes

The nuclear flux of LINERs could easily be contaminated by the light of the underlying host galaxy. Therefore, high angular resolution at all wavelengths is essential. Another complication one should keep in mind is that LINERs could be highly variable on months to years timescales, especially in the UV and X-ray domain (Paper I; Maoz et al. 2005; Pian et al. 2010). Fluxes coming from simultaneous observations are therefore extremely crucial. With these two points in mind, we detail in this section the tools we used to construct the SED of the sources in our sample of LINER 1s with the most reliable multiwavelength data, having simultaneous UV and X-ray fluxes.

To rule out the variability factor, mostly noticeable in the UV and X-ray bands, we used UV observations coming from the optical/UV monitor (OM) telescope, onboard *XMM-Newton*, taken with either the *UVM*2 or the *UVW*2 filters (effective wavelengths of 2310 Å and 2120 Å respectively). These UV fluxes are simultaneous with the *XMM-Newton* X-ray EPIC fluxes. Despite the fact that the angular resolution of the OM is much lower than the *Hubble* Space Telescope (HST) one, LINER sources appear as point-like sources in the UV bands, with the emission of the host galaxy left undetected. Six sources and a total of 7 observations were observed with the OM with either the *UVM*2 or the *UVW*2 filters (NGC 315, obs. ID: 0305290201; NGC 3226, obs. ID: 0101040301; NGC 3718, obs. ID: 0200430501 and 0200431301; NGC 3998, obs. ID: 0090020101; NGC 4143, obs. ID: 0150010601; NGC 4278, obs. ID:0205010101, see Paper I for details on the observation logs), with NGC 315 being the only source observed with both filters. We derive count rates, using the *omsource* interactive photometry tool of the Science Analysis System (SAS), for all of the above mentioned LINER 1s in a circular aperture with a 3″ radius centered on the source. We corrected for the background taken as an annular region with 5″ and 10″ inner and outer radii, respectively. These background-subtracted count rates were then extrapolated to the coincidence-loss area corresponding to 6″ using the point spread function. We converted these count rates to physical fluxes using the two conversion factors of 2.20×10^{-15} erg cm^{-2} Å^{-1} counts^{-1} and 5.71×10^{-15} erg cm^{-2} Å^{-1} counts^{-1} for the *UVM*2 and *UVW*2 filters, respectively[2].

Radio data, whenever possible, are coming from VLBA observations with milliarcsecond resolution. This is important to remove the contamination of any parsec- and/or subparsec-scale jet, detected in the nuclear region of many LINERs. Otherwise, fluxes derived from VLA subarcsecond resolution were used. Infrared data are only accepted when measured with the *Spitzer* telescope with ∼1 arcsec resolution. Even at that resolution, the near-IR (1–3 μm) data could be highly contaminated by the emission from normal stellar populations. The mid-IR (10–30 μm), on the other hand, are more representative of the nuclear emission, although emission from hot dust grains (∼100 K) can potentially contribute to the nuclear flux. Optical data are only taken from the HST with subarcsecond resolution. We complement the SEDs with more HST optical data points by looking at the *Hubble* Legacy Archive (HLA)[3] for any observations with either the WFPC2 or the ACS instruments that were not yet reported in the literature. We use the flux derived from the Virtual Observatory DAOPhot tool in a 0.3″ circular aperture around the LINER 1, originally in counts s^{-1}, and convert it to erg cm^{-2} s^{-1} Å^{-1} by using the PHOTFLAM keyword in the image FITS file. These HLA photometry data are background, charge transfer efficiency, and aperture corrected[4]. Finally, Infrared, optical, and UV data are de-reddened according to the galactic extinctions shown in Table 2, and using the Cardelli et al. (1989) galactic extinction curve.

None of the two OM UV filters encloses the 2500 Å wavelength in order to calculate the optical to X-ray flux ratio, α_{ox} ($\alpha_{ox}= 0.384\ \log(L_{2\ keV}/L_{2500\ Å})$, Tananbaum et al. 1979). Therefore, we derive a 2500 Å monochromatic luminosity from either the *UVM*2 or the *UVW*2 fluxes, assuming a UV spectral index of 0.7 ($F_\nu \propto \nu^\alpha$, where F_ν is in erg s^{-1} cm^{-2}). This UV-spectral index was calculated for NGC 315, which is the only source to be observed with both the *UVM*2 and *UVW*2 filters. In fact, assuming a UV spectral index between 0.4 and 1.0 would only introduce a maximum of 6% error on α_{ox}. Table 1 gives the data points used to construct the SED of the six sources, with simultaneous UV and X-ray fluxes, shown in Fig. 1. Finally, we calculated the bolometric luminosities of these six LINER 1s assuming that two consecutive flux points define a power-law of the form $L_\nu \propto \nu^\alpha$. These bolometric luminosities might be slightly biased by the fact that we know little about LINER sources in the infra-red domain (Fig. 1). However, we expect faint nuclear emission in this energy range in LINER sources since the torus is probably absent (Ho 2008, Paper I).

3.1.1. NGC 315

This immense radio galaxy has been the focal point of many radio studies in the past (Willis et al. 1981; Venturi et al. 1993; Cotton et al. 1999; Canvin et al. 2005; Laing et al. 2006). The radio morphology of NGC 315 indicates a Fanaroff-Riley type 1 (FR I) nucleus with jet structures at both arcsecond and milliarcsecond resolutions. Willis et al. (1981) present arcsecond

[2] http://xmm.esac.esa.int/sas/current/watchout/Evergreen_tips_and_tricks/uvflux.shtml
[3] http://hla.stsci.edu/hlaview.html
[4] http://hla.stsci.edu/hla_faq.html

Table 1. Multiwavelength nucleus data for our sample of LINER 1s.

ν (Hz)	$\log(\nu L_\nu)$ (erg s^{-1})	Aperture (arcsec)	Satellite/Filter	Date	Reference
			NGC 315		
1.41E+15	41.5302	3	OM/*UVW2*	2005 July 02	This work
1.30E+15	41.5514	3	OM/*UVM2*	2005 July 02	This work
5.51E+14	41.2664	0.2	HST/F555W	1998 February 16	González Delgado et al. (2008)
5.47E+14	41.2052	0.2	HST/F547M	1997 June 13	González Delgado et al. (2008)
3.75E+14	41.5289	0.2	HST/F814W	1998 February 16	González Delgado et al. (2008)
8.44E+13	42.0245	2	*Spitzer*/IRAC	2004 July 19	Gu et al. (2007)
6.67E+13	42.1008	2	*Spitzer*/IRAC	2004 July 19	Gu et al. (2007)
5.23E+13	42.2015	2	*Spitzer*/IRAC	2004 July 19	Gu et al. (2007)
3.81E+13	42.3560	2	*Spitzer*/IRAC	2004 July 19	Gu et al. (2007)
1.50E+10	40.8043	0.005	VLBA	1995 April 7	Kovalev et al. (2005)
8.42E+09	40.3053	0.002×0.005	VLBI	1990 November	Venturi et al. (1993)
5.00E+09	40.0919	0.003×0.008	VLBI	1989 April	Venturi et al. (1993)
1.66E+09	39.5398	0.008×0.002	VLBI	1990 September	Venturi et al. (1993)
			NGC 3226		
1.30E+15	40.65	3.0	OM/*UVM2*	2002 March 29	This work
5.47E+14	41.11	0.2	HST/F547M	1997 Mars 18	González Delgado et al. (2008)
9.57E+10	38.73	7.0	NMA/NRO	2002 November 28	Doi et al. (2005)
8.40E+09	37.74	0.004	VLBA	2003 October 2	Anderson & Ulvestad (2005)
4.90E+09	37.20	0.005	VLBA	1997 June 16	Falcke et al. (2000)
			NGC 3718		
1.41E+15	<41.01	3.0	OM/*UVW2*	2004 November 4	This work
6.58E+14	40.52	0.3	HST/F450W	2001 October 03	This work
5.00E+14	41.03	0.3	HST/F606W	2001 October 03	This work
4.55E+14	41.24	0.3	HST/F658N	2004 November 16	This work
4.55E+14	41.46	0.3	HST/F658N	1997 July 17	This work
3.72E+14	40.84	0.3	HST/F814W	2004 November 16	This work
2.31E+11	39.05	1×1	PdBI	2000 December 20	Krips et al. (2007)
1.15E+11	38.64	2×2	PdBI	2000 December 20	Krips et al. (2007)
1.50E+10	37.75	0.15	VLA	1999 September 05	Nagar et al. (2002)
8.40E+09	37.28	0.3	VLA	1999 September 05	Nagar et al. (2001)
5.00E+09	37.08	0.5	VLA	1999 September 05	Nagar et al. (2001)
4.99E+09	37.09	0.006×0.005	EVN	2003 June	Krips et al. (2007)
4.90E+09	36.95	$0.0022 \times 0.001.7$	VLBA	1999 April 01	Nagar et al. (2002)
1.63E+09	36.42	0.008×0.007	EVN	2002 February	Krips et al. (2007)
			NGC 3998		
1.41E+15	41.27	3.0	OM/*UVW2*	2001 May 9	This work
1.20E+15	41.16	0.3	HST/F250W	2002 July 1	Maoz et al. (2005)
9.08E+14	41.16	0.3	HST/F330W	2002 July 1	Maoz et al. (2005)
5.47E+14	41.31	0.2	HST/F547M	1996 March 30	González Delgado et al. (2008)
3.80E+14	41.00	0.2	HST/F791W	1996 March 30	González Delgado et al. (2008)
3.68E+14	41.40	0.2	HST/F814W	2004 March 27	Capetti & Balmaverde (2006)
1.50E+10	38.32	0.1	VLA	1981 March	Hummel et al. (1984)
8.40E+09	38.50	1.0	VLA	1994 April 04	Healey et al. (2007)
5.00E+09	38.52	0.0012	VLBA	2006 May 27	Helmboldt et al. (2007)
			NGC 4143		
1.36E+15	40.13	0.3	HST/F218W	1997 May 30	This work
1.41E+15	40.87	3	OM/*UVW2*	2003 November 22	This work
5.00E+14	40.93	0.2	HST/F606W	2001 February 12	González Delgado et al. (2008)
1.50E+10	37.35	0.15	VLA	1999 September 05	Nagar et al. (2001)
8.40E+09	37.30	0.15	VLA	1999 September 05	Nagar et al. (2001)
5.00E+09	37.11	0.15	VLA	1999 September 05	Nagar et al. (2001)
5.00E+09	37.12	0.0023×0.0012	VLBA	1999 April 1	Nagar et al. (2002)
5.00E+09	36.18	0.071×0.041	MERLIN	2001 October 18	Filho et al. (2006)

resolution observations at 49 and 21 cm of this large radio galaxy. They derive a 49–21 cm constant jet spectral index of $\alpha = -0.6$. Venturi et al. (1993) studied NGC 315 at 18, 6, and 3.6 cm using VLBI networks and found the same spectral index as above between 18 and 6 cm, but it steepens at lower wavelengths (see also Laing et al. 2006). Cotton et al. (1999) explained the sidedness asymmetry in the parse-scale jet in terms of Doppler beaming from an accelerating relativistic jet (see also Canvin et al. 2005). In the infrared, Gu et al. (2007) studied the *Spitzer* images of NGC 315 at 3.6, 4.5, 5.8, and 8.0 μm. The *Spitzer* telescope has a 2″ resolution in these bands, and therefore contamination of the nuclear fluxes by dust emission or even red stars are inevitable. The authors corrected for the background, which basically represent the stellar component, relying

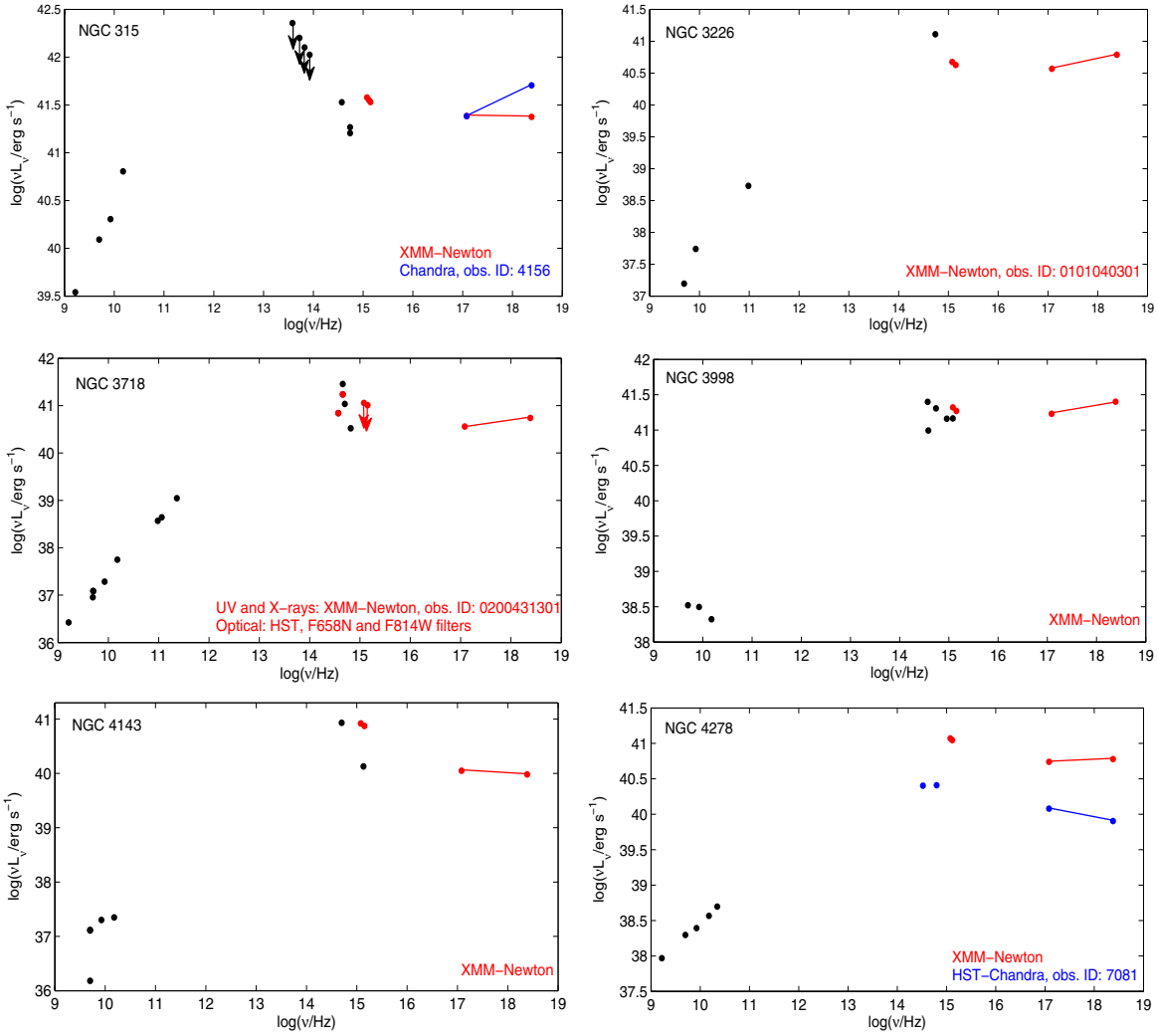

Fig. 1. *Top left panel.* The NGC 315 SED. The red dots represent the simultaneous *XMM-Newton UVM2*, *UVW2*, and X-ray luminosities. The blue dots represent the *Chandra*, obs. ID: 4156, soft and hard band luminosities. Notice the spectral and flux variability in the X-ray band (Paper I). *Top right panel.* The NGC 3226 SED. The red dots represent the simultaneous *XMM-Newton* UV and X-ray luminosities. *Middle left panel.* The NGC 3718 SED, which is one of the most complete SED of our sample with quasi-simultaneous HST-optical and *XMM-Newton* UV and X-ray fluxes (red dots). *Middle right panel.* The NGC 3998 SED with the red dots representing the simultaneous *XMM-Newton* UV and X-ray luminosities. *Lower left panel.* The NGC 4143 SED. The red dots represent the simultaneous *XMM-Newton* UV and X-ray fluxes. Note the high variability amplitude at UV wavelengths between the HST black-dot and the OM red-dots taken six years apart. This LINER 1 shows the highest UV flux relative to the X-ray in our sample. *Lower right panel.* The two NGC 4278 SEDs, representing the low state contemporary HST-optical and *Chandra*-X-ray fluxes (blue dots), and the high state simultaneous *XMM-Newton* UV and X-ray fluxes (red dots). See text for more details.

on the 3.6 μm image (which was shown as a good tracer of the stellar mass distribution in elliptical galaxies, Pahre et al. 2004) between 10″ and 30″. The real challenge is therefore to correct for the heated-dust emission, coming most certainly from the dusty ring seen in the optical band (see below). Gu et al. (2007) demonstrated that the AGN is definitely responsible for some of the emission in the mid-IR band, since its shape is very close to the mid-IR *Spitzer* PSF shape of a point-like source. However, with the current *Spitzer* data set it is difficult to disentangle the dust from the AGN emission. These IR fluxes should then be treated with cautious. At optical wavelength, HST images of NGC 315 show a nuclear compact source surrounded by a nuclear dust disk and chaotic dusty filaments (González Delgado et al. 2008). We calculated two UV fluxes, coming from the *UVW2* and *UVM2* filters, which are simultaneous with the X-ray *XMM-Newton* data. The different fluxes used to construct the NGC 315 SED (Fig. 1) are reported in Table 1. The blue line at X-rays represent the *Chandra*, obs. ID: 4156, fluxes and is only shown for comparison.

We calculate a bolometric luminosity using the *XMM-Newton* absorption corrected luminosities and the data reported in Table 1, only excluding the IR fluxes. We found $L_{\rm bol} = 4.34 \times 10^{42}$ erg s^{-1}. This corresponds to a X-ray bolometric correction $\kappa_{2-10\ {\rm keV}} = L_{\rm bol}/L_{2-10\ {\rm keV}} = 18.3$. We calculate a monochromatic 2500 Å luminosity of about 3.2×10^{26} erg s^{-1} Hz^{-1}. We derive, using this luminosity, an optical to X-ray flux ratio $\alpha_{\rm ox} = -1.15 \pm 0.05$.

3.1.2. NGC 3226

In the radio band, NGC 3226 is detected with the VLBI techniques at milliarcsecond resolution, most likely to be a compact point-like source (Falcke et al. 2000). Nagar et al. (2000) calculated a VLA flux density of 5.4 mJy at 2 cm, which results in a flat radio spectrum between 15 and 5 GHz. Filho et al. (2006) detected NGC 3226 with MERLIN at subarcsec scale and found a peak flux density at 5 GHz of about 3.5 mJy, comparable to the value reported for the VLBA data (see Table 1), therefore,

Table 2. Multiwavelength properties of the different LINER 1s in our sample.

Galaxy name	$E(B-V)_{\rm Gal}$	$\alpha_{\rm ox}$	$\log(L_{2500\ \text{Å}})$ (erg s^{-1} Hz^{-1})	$\log(L_{5\ \rm GHz})$ (erg s^{-1} Hz^{-1})	$R_{\rm X}$	$\log(L_{\rm Edd})$ (erg s^{-1})	$\log(L_{\rm X,crit}/L_{\rm Edd})$	$\log(L_{\rm bol})$ (erg s^{-1})	$\kappa_{2-10\ \rm keV}$
NGC 266	0.069	(...)	(...)	28.08	–2.99	46.54	–6.79	(...)	(...)
NGC 315	0.065	-1.15 ± 0.05	26.50	30.39	–1.54	47.16	–6.90	42.56	15.4
NGC 2681	0.023	(...)	(...)	(...)	(...)	44.88	–6.51	(...)	(...)
NGC 2787	0.131	(...)	(...)	26.89	–1.97	46.25	–6.74	(...)	(...)
NGC 3226	0.023	-1.13 ± 0.04	25.60	27.50	–3.49	46.16	–6.73	41.70	8.3
NGC 3718	0.014	>-1.27	<25.98	27.39	–3.81	45.71	–6.65	41.73	9.8
NGC 3998	0.016	-1.05 ± 0.01	26.24	28.82	–2.79	47.17	–6.90	42.17	5.8
NGC 4143	0.013	-1.37 ± 0.02	25.84	27.42	–2.80	46.28	–6.75	41.54	36.3
NGC 4203	0.012	(...)	(...)	27.39	–3.50	45.83	–6.67	(...)	(...)
NGC 4278	0.029	(...)	(...)	28.60	–2.04	46.82	–6.84	41.25	22.24
	0.029	-1.18 ± 0.02	25.99	28.60	–2.04	46.82	–6.84	41.83	11.25
NGC 4750	0.020	(...)	(...)	(...)	(...)	45.37	–6.59	(...)	(...)
NGC 4772	0.027	(...)	(...)	26.76	–3.39	45.56	–6.62	(...)	(...)
NGC 5005	0.014	(...)	(...)	27.64	–2.74	45.89	–6.68	(...)	(...)

Notes. Columns represent: (1) the galaxy name, (2) the Galactic extinction taken from NED, used to correct the infrared, optical and UV data, (3) the $\alpha_{\rm ox}$ derived for the six LINER 1s with simultaneous UV and X-ray fluxes, (4) the 2500 Å luminosity calculated from either the *UVM2* or the *UVW2* *XMM-Newton*-OM filters in erg s^{-1} Hz^{-1}, (5) the core 5 GHz radio luminosity in erg s^{-1} Hz^{-1}, (6) the radio loudness parameter $R_{\rm X}$, (7) the Eddington luminosity, (8) $\log L_{\rm X,crit}/L_{\rm Edd} = -5.356 - 0.17\log(M/M_{\odot})$ which represents the critical 2–10 keV luminosity above which the broad-band spectrum of a given AGN is thought to become jet-dominated (Yuan & Cui 2005, see Eq. (3)), (9) the bolometric luminosity $L_{\rm bol}$ derived from the SED integration for each of the six LINER 1s with reliable SEDs, and finally (10) the bolometric, hard X-ray, correction $\kappa_{2-10\ \rm keV}$. Two bolometric luminosities were calculated in the case of NGC 4278 corresponding to the low and high state X-ray flux level. See text for details.

Filho et al. (2006) concluded that NGC 3226 does not appear variable at 5 GHz. In the optical band at the HST resolution, NGC 3226 shows an unresolved core surrounded from the eastern side by a dust lane (Martel et al. 2004; González Delgado et al. 2008). In the UV band, NGC 3226 was observed with the *XMM-Newton* OM instrument with the *UVW2* band during only the short observation (obs. ID: 0101040301, see Paper I, the long ~100 ks observation only used the *U* filter, which is highly contaminated by the host galaxy light). The fluxes used to construct the NGC 3226 SED (Fig. 1) are listed in Table 1.

The bolometric luminosity of NGC 3226, derived with the luminosities listed in Table 1 plus the *XMM-Newton* X-ray luminosity, is about 5.1×10^{41} erg s^{-1}. The 2–10 keV luminosity of the *XMM-Newton* (obs. ID: 0101040301) represents 12% of this bolometric luminosity and results in a 2–10 keV bolometric correction $\kappa_{2-10\ \rm keV} \approx 8.4$. From the derived 2500 Å luminosity of about 4×10^{25} erg s^{-1} Hz^{-1}, we calculate a $\alpha_{\rm ox} = -1.13\pm0.04$.

3.1.3. NGC 3718

At 18 cm, with subarcsecond resolution of the MERLIN radio telescope, NGC 3718 shows a compact jet extending to the northwest direction (0.5″), which is weakly present at 6 cm (Krips et al. 2007). The core has a very high surface brightness temperature with a lower limit of 3×10^8 K. It is detected with the VLA and VLBA at subarcsecond and milliarcsecond scales (Nagar et al. 2002). In the optical band, NGC 3718 shows an unusual strongly-warped gas disk (Pott et al. 2004; Krips et al. 2005; Sparke et al. 2009). This gas disk is consistent with the dust lane that goes across the nucleus and seen clearly at the HST resolution. This dust lane makes it very hard to detect the nucleus at optical wavelength and even more in the UV band. In fact, HST UV images of NGC 3718 were blank with no sign of the nucleus to be found (Maoz et al. 1996; Barth et al. 1998). This dust lane is probably responsible for the high internal extinction of about 0.34 mag (Ho et al. 1997a). Therefore, all of the optical and UV fluxes of NGC 3718 were corrected, in addition to the Galactic extinction, for the internal one using the Cardelli et al. (1989) curve.

We calculated optical fluxes coming from HST observations, using the fluxes reported by the DAOPHOT Virtual-Observatory tool of the HLA (see above). In the UV band, NGC 3718 was observed with the OM filter *UVW2* during both *XMM-Newton* observations. The nucleus was not detected so we derived upper limits and corrected these fluxes for Galactic and internal extinction. Table 1 shows the fluxes used to derive the NGC 3718 SED shown in Fig. 1. Luckily, two HST pointings of NGC 3718 were taken almost simultaneously with the *XMM-Newton* observation with almost two weeks separation. These quasi-simultaneous data points are shown in red in Fig. 1.

The NGC 3718 is the most complete SED of our sample with simultaneous data in the optical (HST/F658N/F814W), UV, and X-ray (*XMM-Newton*/0200431301) bands. However, we decided to exclude the UV upper-limit fluxes to calculate the bolometric luminosity of this source, hence, relying only on the detection measurements of the radio and quasi-simultaneous optical and X-ray fluxes (we note here that the UV-flux upper limit is not conflicting with the interpolation between the optical and X-ray fluxes). we find a bolometric luminosity $L_{\rm bol} = 5.43 \times 10^{41}$ erg s^{-1}, resulting in $\kappa_{2-10\ \rm keV} = 10$. We derive an upper limit on the 2500 Å luminosity of about 9.5×10^{25} erg s^{-1} Hz^{-1}, which resulted in a $\alpha_{\rm ox} > -1.26$.

3.1.4. NGC 3998

Hummel et al. (1984) reported a variable radio core at the center of NGC 3998 with a flat spectrum and a very high surface brightness temperature ($>10^8$ K). At milliarcsecond resolution, Filho et al. (2002) reported a weak northern radio extension suspected to be the innermost kpc-scale outflow seen at arcsecond resolution (Hummel 1980). At UV wavelength, Maoz et al. (2005) reported a strong variability between the 5 epoch observations of NGC 3998 with the HST/F250W filter. The flux of the first observation was found the highest and decreasing all along the 4 other observations. Our *XMM-Newton*/OM measurement,

which is a ∼1 year before the first HST observation, is 1.3 times higher (note that our derived *UVW2* flux is consistent with the one derived in Ptak et al. 2004, for the same observation). At optical wavelength with the HST resolution, the nucleus of NGC 3998 is clean as a whistle, not showing any sign of dust lanes or any other source of intrinsic absorption (González Delgado et al. 2008). Table 1 gives the data points used to construct the NGC 3998 SED plotted in Fig. 1.

Using the different radio and optical measurements and the *XMM-Newton* UV and X-ray fluxes we calculate a bolometric luminosity of about 1.5×10^{42} erg s^{-1}. The hard 2–10 keV luminosity is 17% of the bolometric luminosity which results in a $\kappa_{2-10\ \mathrm{keV}} \approx 6$. From the derived 2500 Å luminosity, we calculate a $\alpha_{\mathrm{ox}} = -1.05 \pm 0.01$.

3.1.5. NGC 4143

NGC 4143 has a slightly inverted to flat radio spectrum between 20 cm and 2 cm (Nagar et al. 2000). At the MERLIN resolution of sub-arcsecond, NGC 4143 shows a core emission, lacking any sign of extended jet emission. The core has a high surface brightness temperature of about 2×10^8 K. In the optical band and at the HST resolution, Chiaberge et al. (2005) reports an unresolved nuclear source at the center of NGC 4143, with some weak nuclear dust lanes (González Delgado et al. 2008). We calculated a HST/F218W UV flux for NGC 4143, where the nucleus appears as a point like source. This flux of about 3.94×10^{-13} erg cm^{-2} s^{-1}, is ∼6 times smaller than the flux we derive from the OM/*UVW2* observation taken almost 6 years later. Table 1 presents the NGC 4143 flux points used to derive the SED, shown in Fig. 1.

Using the different radio and optical measurements and the *XMM-Newton* UV and X-ray fluxes we calculate a bolometric luminosity of about 3.5×10^{41} erg s^{-1}. The hard 2–10 keV luminosity is 3% of the bolometric luminosity which results in a $\kappa_{2-10\ \mathrm{keV}} \approx 36$. From the derived 2500 Å luminosity, we calculate a $\alpha_{\mathrm{ox}} = -1.37 \pm 0.02$, the lowest between the six different LINER 1s with a simultaneously measured UV and X-ray flux.

3.2. Optical to X-ray flux ratio, α_{ox}

We report in Table 2 the different values of α_{ox} derived for the six LINER 1s with simultaneous UV and X-ray observations. The values span a range between −1.05 and −1.37. Excluding the lower limit calculated for NGC 3718 of −1.27 would result in a mean of about -1.17 ± 0.02 with a dispersion $\sigma = 0.01$. These values are comparable to the values reported in Maoz (2007, i.e., −0.9-−1.2), for a sample of 13 UV variable LINERs, and Eracleous et al. (2010) for a broad sample of low luminosity AGN, both studies using non-simultaneous UV and X-ray fluxes. However, our α_{ox} values are somewhat lower than the mean value reported in Ho (1999, i.e., −0.9). We attribute this difference to the fact that Ho (1999) used mainly *ASCA* X-ray fluxes derived from large apertures (300″), which would over-estimate the X-ray fluxes and hence the α_{ox} measurements. Moreover, the author sample included both LINERs and low luminosity Seyferts, with α_{ox} values extrapolated from the optical slope at times.

NGC 3998 is the only source our sample shares with the Maoz (2007) sample. The two α_{ox} values are in very good agreement, separated by only 7%. NGC 4143, with a $\alpha_{\mathrm{ox}} = -1.37 \pm 0.02$, is the only source in our sample with a value comparable to values reported for luminous AGN (e.g., Steffen et al. 2006).

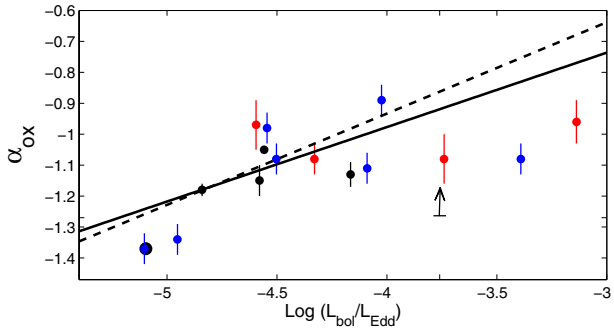

Fig. 2. α_{ox} dependence on the Eddington ratio. The black-dashed line represents the best fit linear regression to our sample of LINER 1s (black dots) and the sample of Pian et al. (2010, red dots), both with α_{ox} values derived from simultaneous UV and X-ray fluxes. The black solid-line represents the best fit linear regression to all data, including the Maoz (2007, blue dots) sample. These latter values derive from non-simultaneous observations. The upper limit represents the value derived on NGC 3718 and is not included in the regression analysis. See text for more details.

This LINER 1 has a comparable 2500 Å luminosity to, but the lowest 2 keV luminosity between, our six LINER 1 sources.

Albeit dealing with a small sample of six LINER 1s, our values of α_{ox} are not subject to uncertainties due to the variability in both UV and X-ray bands. This is a big advantage over the past studies conducted using non-simultaneous data. A similar work has been carried out by Pian et al. (2010), studying the UV to X-ray flux ratio of a sample of four low luminosity AGN with simultaneous UV and X-ray fluxes derived from the *Swift* telescope. NGC 3998, which is one of the four sources of Pian et al. (2010) sample, exhibit a $\alpha_{\mathrm{ox}} = -0.97$, in good agreement with the value we derive here, $\alpha_{\mathrm{ox}} = -1.05$. Recently, Sobolewska et al. (2011) predicted, by simulating the spectra of a sample of AGN based on the evolution pattern of the transient BH binary GRO J1655–40, that the α_{ox}-Eddington ratio relation should change signs at $L_{\mathrm{bol}}/L_{\mathrm{Edd}} \approx 10^{-2}$. This change of sign could represent a switch from a high/soft state to a low/hard state in AGN. Lusso et al. (2010; see also Grupe et al. 2010) found that their sample of type 1 AGN shows an anticorrelation (considering a negative α_{ox}) between α_{ox} and the Eddington ratio. To test the hypothesis of Sobolewska et al. (2011), we plot in Fig. 2 our α_{ox} values (black dots), the results from Pian et al. (2010, red dots), and finally the Maoz (2007, blue dots) results against the X-ray-corrected Eddington ratio ($L_{\mathrm{bol}}/L_{\mathrm{Edd}} = 16 \times L_{2-10\ \mathrm{keV}}/L_{\mathrm{Edd}}$, see Sect. 4, Ho 2008; Paper I). This X-ray-corrected Eddington ratio was used for consistency between the three different works mentioned above. We keep in mind that the Maoz (2007) α_{ox} values derive from non-simultaneous observations, and we excluded the sources with a 2–10 keV flux upper-limit. We would like to emphasize the fact that Maoz (2007) and Pian et al. (2010) samples of LINERs are genuine AGN, since all show short and/or long term UV variability (Maoz et al. 2005).

We find a strong positive correlation (with negative α_{ox} values) between α_{ox} and the Eddington ratio, with and without Maoz (2007) values, confirming the Sobolewska et al. (2011) prediction. A Spearman-rank test gives a 99.3% probability that these two parameters are correlated with a correlation-coefficient $r = 0.64$ (a probability of about ∼95% with a correlation-coefficient $r = 0.62$ if we exclude the Maoz 2007, sample). We performed a simple linear regression analysis weighting by the real measurement errors on α_{ox}, and a mean error of 0.05 in the case of Maoz (2007) values (derived from the individual errors

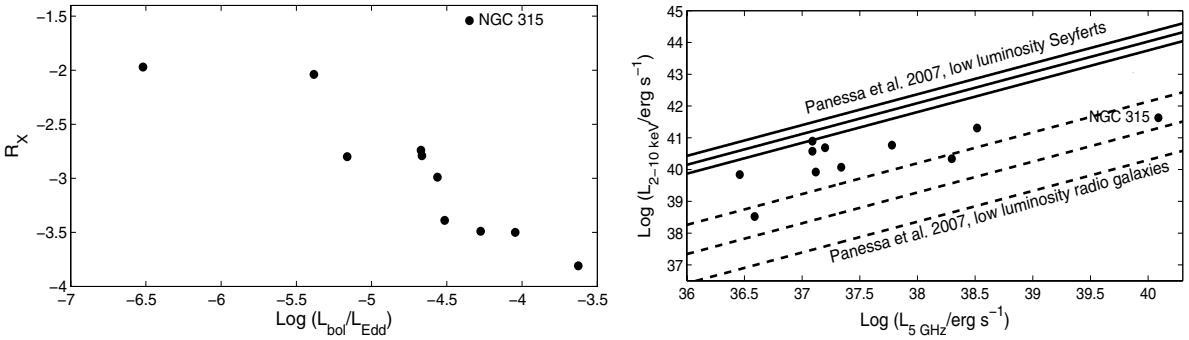

Fig. 3. *Left panel.* The anticorrelation of R_X as a function of the Eddington ratio for the different LINER 1s in our sample. *Right panel.* The positive correlation between the 5 GHz radio luminosity and the hard 2–10 keV luminosity. The solid and dashed lines represent the best fit to a straight line, and the 1σ standard deviation on the intercept, derived for a sample of low luminosity Seyfert galaxies and low luminosity radio galaxies, respectively (Panessa et al. 2007). See text for details.

of our sample and Pian et al. 2010, sample, for the reason of the lack of measurement errors in this latter case), and found that these two parameters follow the equation:

$$\alpha_{ox} = (0.24 \pm 0.07) \log L_{bol}/L_{Edd} - (0.01 \pm 0.31), \quad (1)$$

for the whole sample (solid line, Fig. 2), and

$$\alpha_{ox} = (0.30 \pm 0.10) \log L_{bol}/L_{Edd} + (0.25 \pm 0.45), \quad (2)$$

considering only the α_{ox} derived from simultaneous UV and X-ray fluxes (dashed line, Fig. 2). The errors on the slope and intercept of these relations are at the 68% confidence level (1σ). We deliberately excluded two outliers from the Maoz (2007) sample to perform this analysis: NGC 4552 ($L_{2-10\ keV}/L_{Edd} < 10^{-8}$, $\alpha_{ox} = -1.10$) and NGC 4594 ($L_{2-10\ keV}/L_{Edd} \approx 10^{-7}$, $\alpha_{ox} = -0.92$). These results are discussed in Sect. 5.1.

3.3. Radio loudness parameter, R_X

The radio loudness parameter is usually described as the ratio between the optical luminosity (or the UV luminosity) to the 5 GHz luminosity, $R_o = L_\nu(5\ GHz)/L(B)$ ($R_{UV} = L_\nu(5\ GHz)/L(2500\ Å)$). The barrier separating radio-loud from radio-quiet AGN is defined at $R_{o(UV)} = 10$. Another alternative, better suited to calculate the radio loudness of LLAGN, is to use the hard 2–10 keV X-ray luminosity, $R_X = \nu L_\nu(5\ GHz)/L_{2-10\ keV}$ (Terashima & Wilson 2003). This radio loudness parameter has many advantages over its predecessor in the case of LLAGN. Indeed, as stressed by Terashima & Wilson (2003), the optical luminosity of LLAGN could easily be contaminated by circumnuclear emission, e.g., from stars. Moreover, one has to be careful correcting for extinction from the circumnuclear dust present at the center of a number of low luminosity AGN. The hard X-ray luminosities are basically insensitive to large X-ray obscuration ($N_H \leq 10^{23}$ cm^{-2}) and the hard X-ray emission is commonly believed to be the intrinsic AGN emission. Following this criteria, Terashima & Wilson (2003) showed that log $R_X = -4.5$ would be the barrier separating radio-loud (log $R_X > -4.5$) from radio-quiet AGN.

Eleven sources in our sample have 5 GHz luminosities coming from either VLA or VLBA observations (NGC 2681 and NGC 4750 were not detected, Nagar et al. 2005). We report in Table 2 the different log R_X values for the different 11 LINER 1 sources. Since the X-ray and radio observations were never simultaneous, we decided to use the arithmetic mean X-ray luminosities of the sources with multiple X-ray observations (Paper I), keeping in mind that variability in both bands may introduce some scatter on the derived values. We find a log $R_X > -4.5$ in all of the cases with a geometric mean value of -2.7. According to Terashima & Wilson (2003) criterion, all of the 11 LINER 1s with detected 5 GHz core could be considered as radio-loud sources[5]. However, Panessa et al. (2007) studied a sample of low luminosity Seyfert galaxies (type 1 and type 2) and a sample of low luminosity radio galaxies. They found a bimodality in the distribution of both R_o and R_X between the two classes and hence re-calculated, based on the assumption that Seyfert galaxies are radio-quiet objects, the boundary between radio-loud and radio-quiet sources to be log $R_o > 2.4$ and log $R_X > -2.8$. Based on this assumption, 6/11 LINER 1s would be considered as radio-loud sources. The remaining five sources would be considered as intermediate-radio sources with log R_X ranging between -3 and -3.5 (except for NGC 3718 that exhibits a mean log $R_X \approx -3.8$).

Ho (2002) found a strong anticorrelation between the radio-loudness parameter R_o and the Eddington ratio for a sample of AGN spreading over almost 10 orders of magnitude in Eddington ratio space (see also Sikora et al. 2007). We show in the left panel of Fig. 3 the dependence of the radio loudness parameter, R_X, on the Eddington ratio. There is clearly a strong anticorrelation between the two parameters. Panessa et al. (2007) found the same anticorrelation when considering the R_X parameter for a sample of low luminosity Seyfert galaxies and low luminosity radio galaxies. Here, we establish this correlation for the first time for LINER 1s. We find a Spearman rank correlation coefficient $r = -0.71$ and a probability of 98.5% that these two parameters are correlated. NGC 315, which is the only FR I radio galaxy in our sample clearly does not follow the same anticorrelation. Radio galaxies (i.e., FR I radio galaxies, radio-loud quasars, and broad-line radio galaxies) follow their own anticorrelation in Eddington-ratio–R_o space (Sikora et al. 2007), and probably their own anticorrelation in Eddington-ratio–R_X space. Therefore, excluding NGC 315 from the data would result in a Spearman-rank correlation coefficient $r = -0.95$ and a probability >99.99% that these two parameters are correlated.

Finally, Panessa et al. (2007) found a strong positive correlation between the hard 2–10 keV luminosity and the radio luminosity at 6 cm for a sample of low luminosity Seyfert galaxies (see also de Gasperin et al. 2011) and a sample of low luminosity radio galaxies. We show in the right panel of Fig. 3 the

[5] We note that we find a $R_{UV} > 40$ for the six sources in our sample with derived UV luminosities, hence, according to the classical classification criterion these LINER 1s would be considered as radio-loud sources.

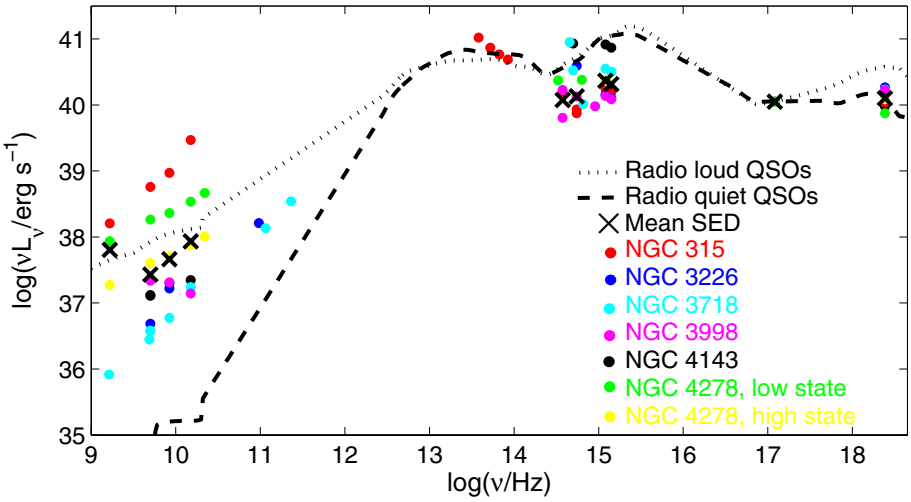

Fig. 4. The SEDs of the six different LINER 1s in our sample with simultaneous UV and X-ray fluxes (different colored-dots) plotted alongside their geometric mean SED (black crosses) and the mean SED of a sample of radio-quiet and radio-loud AGN (Elvis et al. 1994). See text for more details.

dependence of the mean hard X-ray luminosity of our sample of LINER 1s on the 6 cm radio luminosity. According to the Spearman-rank test, these two parameters are positively correlated with $r = 0.69$ and $p = 99\%$. The best fits to a straight line derived by Panessa et al. (2007) on both low luminosity Seyfert and radio galaxies are shown as solid and dashed lines, respectively, with the 1σ standard deviation on the intercepts. Our LINER 1 sample clearly populate the region between the Panessa et al. (2007) two best fit lines, indicating that LINER 1s, and all AGN-powered LINERs by extrapolation, are more radio-loud, for a given X-ray luminosity, than low luminosity Seyfert galaxies and less radio-loud than low luminosity radio galaxies. All these results are discussed in Sect. 5.2.

4. Properties of LINER 1 SEDs

In order to get a better insight on our LINER 1 SEDs, compare them to each other and to more luminous AGN, we overplot in Fig. 4 the SED of the six different LINER 1s, after normalizing them to the 0.5–2 keV luminosity of NGC 4143 (different colored-dots represent different SEDs, see figure legend). The choice of NGC 4143 is somewhat arbitrary and was preferred for having the lowest 0.5–2 keV luminosity (our conclusions would not, in any way, be affected by the choice of the normalizing source). Two SEDs were reported in the NGC 4278 case, one corresponding to the high state simultaneous X-ray and UV *XMM-Newton* fluxes and one representing the contemporary HST-optical and *Chandra*-X-ray (obs. ID: 7081) fluxes (see Younes et al. 2010). We decided to normalize all SEDs preferentially at the X-ray luminosity, since our main focus is the validity of a "big blue bump" at UV wavelength relative to the X-ray emission, plus to check whether they are to be considered radio-loud or radio-quiet sources relative to X-rays. For comparison purposes, we plot the Elvis et al. (1994) average SED of a sample of radio-loud and radio-quiet AGN (dotted-line and dashed-line, respectively; we note that Shang et al. 2011, found that the overall shape of the average SED of their sample of radio-quiet and radio-loud AGN, compiled using high-quality multiwavelength data from space-based and ground-based telescopes, is very similar to the Elvis et al. 1994, SEDs compiled almost two decades ago). Finally, we add the geometric[6] mean SED (black crosses, the geometric mean minimizes the effect of extreme outliers) that we calculated whenever we have three or more data points of different sources at a given frequency ν_0. To make use of the data as much as possible, a flux data-point, at radio or optical wavelength, measured at a frequency ν_1, in the interval between $\nu_0 - 0.1$ dex and $\nu_0 + 0.1$ dex, was considered as calculated at ν_0. In other words, we consider a source to have a flat spectrum in a frequency interval of 0.2 dex (we note that modeling the SEDs with accretion/jet models is out of the scope of this work and will be treated in a forthcoming paper).

The different properties of the SEDs of our sample of LINER 1s, and the property of the mean SED, which represents to some extent LINER 1s as a class and all AGN-powered LINERs by extrapolation, compared to the SED of radio-quiet and radio-loud quasars could be summarized as follows:

1. At radio wavelength and for a given X-ray luminosity, all of the six LINER 1s in our sample present a radio emission at least an order of magnitude larger than that of radio-quiet quasars. Two of the sources, NGC 315 and NGC 4278, exhibit radio emission comparable to radio-loud quasars. The radio-loudness parameter R_X indicates that all of the six LINER 1s could be considered as radio-loud sources having $\log R_X > -4.5$ (see Sect. 3.3).
2. At a given X-ray luminosity, the geometric-mean optical and UV fluxes are 5 to 10 times, respectively, weaker than the optical and UV emission of both radio-quiet and radio-loud quasars. This leads to an optical-to-X-ray flux ratio $\alpha_{ox} \approx -1.17 \pm 0.02$ (see Sect. 3.2), compared to mean values of about -1.3 and -1.5 for Seyferts and quasars, respectively (Mushotzky & Wandel 1989; Brandt et al. 2000; Steffen et al. 2006; Lusso et al. 2010). Consequently, the "big blue bump", clearly seen in the SED of quasars, is much less apparent in the SED of our sample of LINER 1s.
3. In the X-ray band, the geometric mean spectrum in νL_ν space is flat and hence comparable to those of radio-quiet AGN. This is quite a surprise since in the radio-band these sources have radio luminosities, normalized to the X-ray band, comparable to those of radio-loud quasars. In fact, the radio loud quasars have an average X-ray photon index of about $\Gamma \approx 1.5$ (e.g., Worrall & Wilkes 1990; Yuan et al. 1998; Reeves et al. 1997; Reeves & Turner 2000; Gambill et al. 2003; Belsole et al. 2006; Miller et al. 2011), resulting from either X-rays dominated by synchrotron emission from a jet or the consequence of X-ray beaming effects. The X-ray spectral shape resemblance that our LINER 1s (with an average $\Gamma = 1.9$, see Paper I) share with radio-quiet quasars, and also Seyfert

[6] The geometric mean of a vector $X = [X1, X2, ..., Xn]$ is defined as $(\prod_{i=1}^{n} X_i)^{1/n}$.

galaxies (Nandra et al. 1997; Porquet et al. 2004), could point toward an accretion flow origin rather than a jet-origin for the X-ray emission.

4. Finally, we would like to note here that the bolometric luminosities of these LINER 1s, derived from their SED, are extremely low compared to luminous AGN. These bolometric luminosities vary between 2×10^{41} and 4×10^{42}, resulting in Eddington ratios between 10^{-4} and 3×10^{-6}. The hard X-ray luminosities present 3% to 17% of these bolometric luminosities and result in an average 2–10 keV bolometric correction, $\kappa_{2-10\,\mathrm{keV}}$, of about 16. This value is equal to the one reported in Ho (2008, $\kappa_{2-10\,\mathrm{keV}}\approx16$), and is smaller than the values reported for more luminous AGN (i.e., ~30), in agreement with the anticorrelation found between $\kappa_{2-10\,\mathrm{keV}}$ and the Eddington ratio (e.g. Vasudevan & Fabian 2009).

5. Discussion

We have shown in Paper I that AGN-powered LINERs, based on their X-ray temporal and spectral properties, might have a different accretion mode than the one thought to exist in luminous AGN. Briefly, we have shown that, (1) fast X-ray variability (hours to days) is rare in these sources, (2) the X-ray spectral features defining most luminous AGN are absent in LINER 1s (e.g., Fe Kα, soft excess below ~2 keV), and (3) the X-ray photon index Γ is anticorrelated to the Eddington ratio, which could be interpreted as the increase in the optical depth of a RIAF with increasing Eddington ratio leading to the hardening of the X-ray spectrum. In this work, we complement Paper I by studying the multiwavelength properties of the same sample of LINER 1s. In the following, we discuss our results in the framework of accretion mechanisms and radiative processes taking place in LINER 1s, hence all AGN-powered LINERs by extrapolation. We seek answers by comparing LINER 1s multiwavelength properties to the properties of luminous AGN and the behavior of transient XRBs.

5.1. The enigma of a standard accretion disk in LINERs

The standard geometrically thin accretion disk model emits most of the energy in the UV in the case of a BH with a $\sim10^6$–$10^9\,M_\odot$. This is in line with the observations of Seyferts and quasars, which show a "big blue bump" at UV wavelengths in their SEDs. The bump translates into a UV to X-ray flux ratio, α_{ox}, in the range between −1.3 to −1.5. This UV to X-ray flux ratio, α_{ox}, is an essential tool in order to understand the link between the UV and X-ray emission and to test accretion mechanisms and radiative processes in AGN. The sparse studies of α_{ox} in low luminosity AGN, including LINERs, showed that this class of faint AGN show larger α_{ox} values and hence a shallower UV "big blue bump". Ho (1999) derived an average value for α_{ox} of about −0.9 for his sample of seven low luminosity AGN, somewhat larger than the value we report here (−1.17). The UV and X-ray flux ratios were not simultaneous, plus, their X-ray fluxes were coming from low spatial resolution observations with apertures as big as 300″. Maoz (2007; see also Eracleous et al. 2010), calculated the α_{ox} of a sample of 13 LINERs (being of type 1 or type 2) showing UV variability on time-scales of years. He found an average value of almost −1.13. This value is somewhat consistent with Ho (1999) and in very good agreement with our results that show a mean value of about -1.17 ± 0.02, which is based on simultaneous UV and X-ray observations.

Many studies in the past showed that α_{ox} is strongly anticorrelated to the monochromatic 2500 Å luminosity in classical AGN (Zamorani et al. 1981; Avni & Tananbaum 1982; Vignali et al. 2003; Strateva et al. 2005; Steffen et al. 2006; Kelly et al. 2007; Lusso et al. 2010; Kelly et al. 2010; Grupe et al. 2010). This means that the prominent UV "big blue bump" seen in quasars, which result in an average $\alpha_{ox}\approx-1.4$ (e.g., Elvis et al. 1994), tend to vanish at very low UV luminosities. Maoz (2007; see also Pian et al. 2010), by showing that the α_{ox} values of his sample follows the same $\alpha_{ox}-L_{2500\,\text{Å}}$ anticorrelation shared by Seyferts and quasars (Steffen et al. 2006), suggested that a geometrically thin accretion disk could survive very low accretion rates. Additionally, Maoz (2007) showed that the α_{ox} value of his sample are similar to values reported for AGN of X-ray luminosities ranging from 10^{41} erg s^{-1} to 10^{43} erg s^{-1} and having low BH masses ($\sim10^6\,M_\odot$). These low BH-mass AGN have a mean α_{ox} of about −1.2 (Greene & Ho 2007).

The BH mass appears to be an essential parameter in the accretion physics around BHs. Indeed, the hard 2–10 keV luminosity is positively correlated to the BH mass (Ho 2009), and hence α_{ox} should be BH mass dependent. Kelly et al. (2008) showed that, for a large sample of 318 radio quiet quasars, α_{ox} is strongly anticorrelated with the BH mass (note here that we are assuming negative α_{ox} values, not the other way around as treated by the authors). They were able to explain such a dependence with a UV to X-ray spectrum inferred from a simple model describing the standard geometrically thin accretion disk. This last anticorrelation explains the high α_{ox} values calculated for the low BH-mass AGN of Greene & Ho (2007) in the framework of a geometrically thin accretion disk. However, the BH masses of the samples of Maoz (2007), Pian et al. (2010), and this work lie in an interval between $10^7\,M_\odot$ and $10^9\,M_\odot$. These masses should result in a α_{ox} between −1.24 and −1.58 (Kelly et al. 2008). Fifteen out of nineteen in these three samples have α_{ox} greater than −1.2, hence, inconsistent with the above interval.

Return to the $\alpha_{ox}-L_{2500\,\text{Å}}$ anticorrelation, Sobolewska et al. (2011) showed that, by simulating the spectra of a sample of AGN based on the evolution pattern of the transient BH binary GRO J1655–40, LINERs roughly follow the dependence of α_{ox} on the optical luminosity of AGN. Nonetheless, the authors showed that LINERs should be in a low/hard state to exhibit the observed low optical luminosities, $\log(\nu L_\nu)_o\approx39.5$–$41.3$, again, considering their relatively high BH masses, 10^7–$10^9\,M_\odot$.

Sobolewska et al. (2011) predicted a change in the sign of the α_{ox}-Eddington ratio relation below $L_{bol}/L_{Edd}\approx10^{-2}$, where these two parameters become positively correlated (considering negative α_{ox}). This change would correspond to a switch from a high/soft to a low/hard state in transient XRBs. We confirm in Sect. 3.2 the Sobolewska et al. (2011) prediction and we show in Fig. 2 the positive α_{ox}-Eddington ratio correlation that we establish for a sample of AGN-powered LINERs. This correlation is in contrast with the one found for luminous AGN (Lusso et al. 2010; Grupe et al. 2010). Overplotting our positive correlation with the anticorrelation found by Lusso et al. (2010) for a sample of type 1 AGN (Fig. 5), we find that the switch from a high/soft state to a low/hard state in AGN might occur at the transitional point corresponding to $L_{bol}/L_{Edd}\approx10^{-2.8}$ and a α_{ox} of about −0.7. This Eddington ratio limit that separates two different radiative behaviors between luminous AGN and LLAGN has been reported in the past using the dependence of the X-ray photon index, Γ, on the Eddington ratio. Paper I (see also Gu & Cao 2009) predicted that below a similar Eddington ratio value ($L_{bol}/L_{Edd}\approx10^{-2.6}$), LINER 1s might have a RIAF accretion flow instead of a thin accretion disk to explain the $\Gamma-L_{bol}/L_{Edd}$

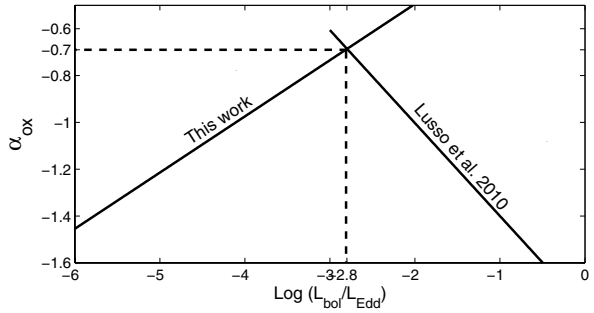

Fig. 5. Positive and negative correlations between α_{ox} and the Eddington ratio for our sample of AGN-powered LINERs (Sect. 3.2) and a sample of type 1 AGN (Lusso et al. 2010), respectively. The crosspoint at $L_{bol}/L_{Edd} \approx 10^{-2.8}$ might suggest a transition from a high/soft state AGN where a thin accretion disk exists to a low/hard state LLAGN where a RIAF forms.

anticorrelation, which is in contrast to the one observed in luminous AGN (Shemmer et al. 2008, and references therein). Additionally, we would like to point out that very recently, Xu (2011) reached similar results when considering a sample of 49 LLAGN, including 21 LINERs, that exhibit $L_{bol}/L_{Edd} < 10^{-3}$. In contrast to our work, where UV luminosities are derived directly from UV observations plus being simultaneous to X-rays, the author derived the 2500 Å luminosities for their sources by extrapolating the B band optical luminosity, calculated either directly or indirectly (using the luminosities of the Hα and/or Hβ lines). Nevertheless, the slope of the correlation that Xu (2011) found (0.163) is in good agreement, within the error bars, with our result. Xu (2011) was able to "roughly" reproduce the correlation using the advection dominated accretion flow (ADAF) model. In ADAFs, the optical/UV luminosity is the result of inverse Compton scatter of the soft synchrotron photons by the hot electrons in the flow. The X-ray photons result from second order inverse Compton of soft synchrotron photons by the hot electrons and from bremsstrahlung processes. At high accretion rates (which is conservatively equivalent to the Eddington ratio), the inverse Compton component dominates the X-ray spectrum. With decreasing accretion rate, the inverse Compton component becomes softer (due to the decrease in the Compton y-parameter, Paper I), and X-ray photons result only from bremsstrahlung process. Hence, the X-ray flux will decrease faster than the UV flux with decreasing accretion rate (see Fig. 5 of Xu 2011, where the author plots the ADAF predictions for three different accretion rates of a given BH mass), resulting in the above seen α_{ox}-Eddington ratio correlation. This last point adds to the long list of evidence supporting RIAFs as accretion-mode candidates in LLAGN.

Finally, we have stated in Sect. 3.2 that we have excluded two LINERs from Maoz (2007) sample that clearly diverge from the α_{ox}-Eddington-ratio relation. These two LINERs are the faintest between all LINERs considered here, having the lowest $L_{2-10\,keV}/L_{Edd}$ ($<10^{-7}$), but with a somewhat high α_{ox} (>-1.1). Three possibilities emerge: (1) this is due to the variability factor since the UV and X-ray fluxes of Maoz (2007) were non-simultaneous, (2) the UV emission of these two sources is heavily internally absorbed, hence correcting for internal extinction would drive the α_{ox} to lower values, or (3) the α_{ox}-Eddington-ratio relation breaks at very low $L_{2-10\,keV}/L_{Edd}$ ($\lesssim 10^{-7}$), i.e., during the quiescent state of AGN. This would imply that a different radiative process is taking place at such very low Eddington ratios. This latter speculation is interesting to the fact that Yuan & Cui (2005, see also Sect. 5.3) predicted that under a critical $L_{2-10\,keV}/L_{Edd}$ of about $\sim 10^{-6}$, i.e., during the quiescent state of AGN, the jet emission should dominate over the RIAF from radio to X-rays. A bigger sample of AGN with very low $L_{2-10\,keV}/L_{Edd}$ would help confirm or refute this hypothesis.

5.2. Radio emission in LINERs and the role of the jet

It is now believed that radio emission is a common characteristic of low luminosity AGN in general and LINERs specifically (Nagar et al. 2000; Falcke et al. 2000; Nagar et al. 2001, 2002, 2005). For a given X-ray or UV emission, the radio luminosities of these type of objects compare well with radio-loud sources, and exhibit radio-loudness parameters, $R_{o(UV)}$ and R_X, that belong to the radio-loud population of AGN (Ho 1999, 2002; Maoz 2007; Eracleous et al. 2010). Our SED analysis strengthen this idea, as we show that the radio-loudness parameter R_X indicates that all of our 11 LINER 1s with 5 GHz detection could be considered as radio-loud sources according to the Terashima & Wilson (2003) criterion, $\log R_X > -4.5$.

The emission processes of such a radio emission is not yet firmly understood, though more and more hints are pointing towards a jet and/or outflow synchrotron origin. Di Matteo et al. (2001) showed that synchrotron emission of the thermal relativistic electrons in a hot accretion flow (e.g., RIAF) overestimates the radio emission of the nuclei of his sample of four elliptical galaxies. The authors assumed an accretion rate in the RIAF equal to the Bondi accretion rate calculated from the typical temperatures and densities of the hot gaseous halos surrounding their sample nuclei. Even with an accretion rate much less than the Bondi rate, the radio spectral shape is inconsistent with the RIAF prediction. However, if the accretion flow produces outflows and/or jets in the inner regions, as is expected from RIAF models (Narayan & Yi 1995a; Blandford & Begelman 1999), emitting synchrotron non-thermal emission, the radio spectral shape and luminosities reconcile with the observations. Ulvestad & Ho (2001) came to the same conclusion when studying the radio emission of three low luminosity AGN observed at 4 radio wavelengths. Moreover, Nagar et al. (2001) carried out a similar analysis performed on a bigger sample of 16 low luminosity AGN. They found that a jet model is a better explanation than a RIAF model of the flat radio spectra. In fact, a large fraction of LINERs and low luminosity AGN have flat spectra in the radio band (e.g., between 2 and 20 cm, Nagar et al. 2002; Anderson et al. 2004), and some even exhibit subparsec scale radio jets (Falcke et al. 2000).

Ho (2002) found a strong anticorrelation between the radio-loudness parameter R_o and the Eddington ratio for a sample of low luminosity and normal luminous AGN spreading over almost 10 orders of magnitude in Eddington ratio space (see also Sikora et al. 2007). Panessa et al. (2007) confirmed the same anticorrelation for their sample of low luminosity Seyferts when considering the R_X parameter. We find in this work that $\log R_X$ is highly anticorrelated with $L_{2-10\,keV}/L_{Edd}$ for our sample of LINER 1s (Fig. 3, we will discuss the case of NGC 315, which is the only outlier compared to the rest of our sample, later this section), thus stretching this anticorrelation to include LINER 1s specifically, and AGN-powered LINERs in general. This behavior is perfectly in line with the prediction of RIAF structure to produce and collimate relativistic jets more efficiently with decreasing Eddington ratio.

Panessa et al. (2007) found a positive correlation between the hard X-ray luminosity and the 5 GHz radio luminosity for their sample of low luminosity Seyfert galaxies with a slope of 0.97. To compare their results to radio galaxies, the authors collected radio and X-ray luminosities for a sample of LLRGs

from Chiaberge et al. (2005) and Balmaverde et al. (2006). They found that LLRGs show, similar to low luminosity Seyferts, a positive correlation with a slope of 0.97 but three orders of magnitude shifted towards radio luminosities (Fig. 3). Panessa et al. (2007) pointed out the presence of a gap between the two populations clearly seen in $L_r - L_X$ space (Fig. 3). These putative objects, as noted by the authors, are none other than LINERs. This is shown in the right panel of Fig. 3 where the majority of our LINER 1s populate the space between the two best fits of low luminosity Seyferts and LLRGs (again, with the exception of NGC 315, which clearly belongs to LLRGs). Although our small number of 11 LINER 1s makes it difficult to perform rigorous statistical analysis, we find, using a simple linear regression analysis, that $\log L_X \propto (0.8 \pm 0.2) \log L_r$ (excluding the NGC 315 radio galaxy would result in $\log L_X \propto (1.1 \pm 0.3) \log L_r$), which is in agreement, within the error bars with the slope found for both samples of Panessa et al. (2007). Bigger samples of LINERs would be better suited for such analysis. Nonetheless, similar slopes were found for a sample of low-power radio galaxies with X-ray data taken from *ROSAT* (Canosa et al. 1999) and for the radio-quiet sample of Brinkmann et al. (2000, a steeper slope of 0.5 was found for their radio-loud AGN). Such correlations could only mean that a coupling between the radio emission mechanism and the X-ray emission mechanism exists. Whether both emissions emanates from the same origin (i.e., jet), or emanates from different origins although highly coupled (i.e., jet-RIAF) is a highly debated subject, which brings us to the "fundamental plane of BH activity", a reliable tool to distinguish X-ray processes of different accreting BHs.

Finally we would like to give our thoughts on the special case of NGC 315. The LINER 1 NGC 315 is the only source in our sample to be classified as a radio galaxy (FR I morphology), showing an arcsecond scale radio and X-ray jet. It also harbors the second most massive BH in our sample with $M_{BH} > 10^9\ M_\odot$. NGC 315 clearly does not follow the anticorrelation shared by the other LINER 1s between the radio-loudness, R_X, and the Eddington ratio (Fig. 3). This behavior of radio galaxies to occupy a parallel, towards radio-louder systems, anticorrelation in the radio-loudness–Eddington-ratio space was noticed by Sikora et al. (2007). The BH mass has been attributed in many studies as a major factor behind the dichotomy in the strength of the radio emission between radio galaxies and normal AGN, with the most massive BHs resulting in radio-loud sources (e.g., Laor 2000; Dunlop et al. 2003). Indeed, Broderick & Fender (2011) showed that the two populations of Sikora et al. (2007) almost overlap if the BH mass is taken into account and only the core radio emission is considered. However, Ho (2002) noted that radio-loud sources could be present at the center of AGN harboring BHs of very low masses ($10^6\ M_\odot$), plus relatively radio-quiet sources could be present in AGN with BH masses $>10^9\ M_\odot$ (e.g., NGC 3998). Sikora et al. (2007) introduced the BH spin along with the BH mass as a driver of the radio-loudness in AGN (as has been proposed in the past, Blandford 1990; Wilson & Colbert 1995; Meier 1999). Indeed, FR I radio galaxies, to which NGC 315 belongs, are believed to have rapidly spinning BHs (Wu et al. 2011). Consequently, the BH mass, the BH spin, and the Eddington ratio might be behind the dichotomy between radio-quiet and radio-loud AGN.

5.3. Fundamental plane of LINER 1s, RIAF versus jet

It has been almost 8 years now since the discovery of the fundamental plane of BH activity uniting, X-ray luminosities, radio-luminosities, and BH masses of different types of accreting BHs, being stellar or supermassive, thanks to the pioneering work of Merloni et al. (2003). Since then, numerous articles have seen the light as a complement or to better constrain the coefficients of such a fundamental plane (Körding et al. 2006; Wang et al. 2006; Li et al. 2008; Gültekin et al. 2009; Yuan et al. 2009; Plotkin et al. 2012, to name a few). Merloni et al. (2003) used a large sample of different classes of accreting BHs, including XRBs (being in both low/hard and high/soft states), low luminosity AGN, Seyferts, and quasars. They found that the coefficients of their "fundamental plane" could be reproduced in a RIAF context at the 1 sigma confidence level. A geometrically thin accretion disk is excluded at the 3 sigma level, whereas a jet is roughly consistent with the data at the 3 sigma level. Mixing quasars, Seyferts, and high/soft state XRBs with low luminosity AGN and low/hard state XRBs could be misleading. XRBs in their low/hard state show a very strong radio and X-ray correlation, which breaks when these XRBs are in a high/soft state (e.g., Fender et al. 1999). Moreover, Seyferts and quasars are thought to have a X-ray emission mechanism different than the one thought to exist in low luminosity AGN (Paper I). This could, in part, explain the relatively large scatter around the coefficients of the authors fundamental plane. At the time of the Merloni et al. (2003) discovery, Falcke et al. (2004) showed that his sample of Galactic BH binaries in the low and quiescent state, LINERs, FR I radio galaxies, and BL Lac objects (i.e., low Eddington ratio radio galaxies with the jet aligned with our line of sight) can be unified on a 3D plane, none other than the fundamental plane. The authors explained the scaling coefficients of their relation with the analytical solution of a jet model. The fundamental plane discovery, in itself, is a gigantic step towards understanding accretion processes and emission mechanisms giving rise to the radio and X-ray luminosities. Thus, refining the plane with less scatter around the coefficients is crucial to distinguish between the different accretion models in low accreting BHs, mainly between the two most competing ones "RIAF versus jet".

Our small sample of 10 LINER 1s[7] with detected 5 GHz cores do not allow us to perform a rigorous fundamental plane analysis. Therefore, in order to infer the X-ray emission mechanism and to favor a RIAF or a jet model over the other, we relied on two different works: Yuan et al. (2009) and Plotkin et al. (2012).

Yuan et al. (2009) studied the fundamental plane of 22 low luminosity AGN with X-ray luminosities below a critical value $L_{X,crit}$, defined as:

$$\log\left(\frac{L_{X,crit}}{L_{Edd}}\right) = -5.356 - 0.17 \log\left(\frac{M}{M_\odot}\right), \quad (3)$$

below (above) which the X-ray emission should be jet (RIAF) dominated, according to the Yuan & Cui (2005) prediction. Yuan et al. (2009) found that their sample of LLAGN with X-ray luminosities below the critical value, hence jet-dominated, follows the relation

$$\log L_R = 1.22\ \log L_X + 0.23\ \log M_{BH} - 12.46. \quad (4)$$

Recently, Plotkin et al. (2012; see also Körding et al. 2006) calculated the fundamental plane of a well defined sample of XRBs in their low/hard state, low luminosity AGN and BL Lac objects.

[7] We decide to exclude the FR I radio galaxy NGC 315 from this analysis since these sources are not appropriate to test the jet-only model, for the reason of synchrotron cooling occurring at very low frequencies (Fossati et al. 1998; Körding et al. 2006).

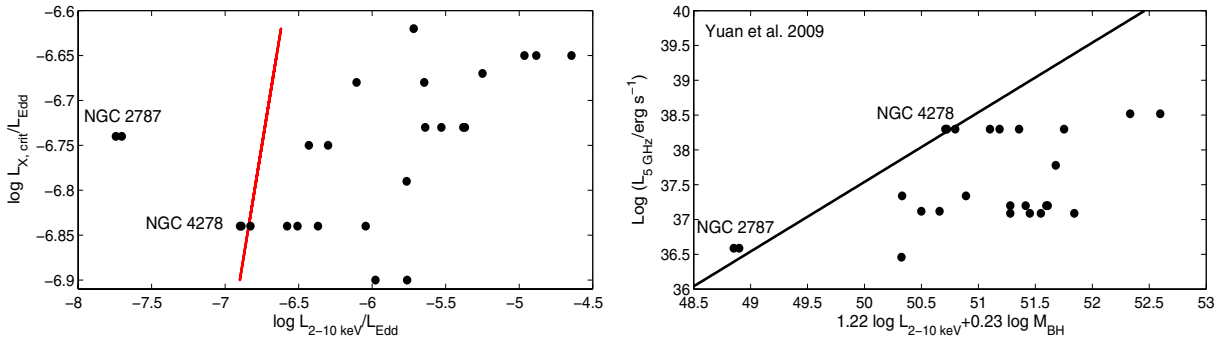

Fig. 6. *Left panel.* Solid line represents the distribution of the critical X-ray luminosity, $L_{\rm X,crit}/L_{\rm Edd}$, below (above) which the X-ray emission is thought to be jet (RIAF) dominated (Yuan & Cui 2005). Black dots represent the distribution of $L_{2-10\ \rm keV}/L_{\rm Edd}$ for our sample of 10 LINER 1s (Paper I). Only NGC 2787 and the three lowest flux NGC 4278 observations have lower $L_{2-10\ \rm keV}/L_{\rm Edd}$ than the critical one. *Right panel.* Our LINER 1s data points superimposed over the Yuan et al. (2009) fundamental plane (black solid line). Only the observations with $L_{2-10\ \rm keV}/L_{\rm Edd} < L_{\rm X,crit}/L_{\rm Edd}$ follow the authors fundamental plane, in perfect agreement with their prediction. See text for more details.

They used a rigorous statistical method based on a Bayesian regression to calculate the errors on the coefficients and the dispersion of their equation. Their fundamental plane follows the equation:

$$\log L_{\rm X} = 1.45\ \log L_{\rm R} - 0.88\ \log M_{\rm BH} - 6.07, \quad (5)$$

with a dispersion $\sigma = 0.07$ dex[8]. The authors found that the coefficients of the fundamental plane of their sample are very well explained with a jet model (the scale-invariant jet model, Heinz & Sunyaev 2003) and that a RIAF model (ADAF solution, Narayan & Yi 1994) is excluded at the 3 sigma level.

We first plot in the left panel of Fig. 6 the distribution of the critical X-ray luminosities (red solid line, see also Table 2) of the different LINER 1s in our sample, below (above) which the X-ray emission should be jet (RIAF) dominated, according to Yuan & Cui (2005). We overplot the X-ray luminosities of the different X-ray observations of our sample (black dots, see Paper I for the different X-ray luminosities of our sample). The left panel of Fig. 6 shows that only NGC 2787 and the three *Chandra* observations of NGC 4278 with the lowest fluxes (obs. IDs: 7077, 7080, and 7081, see Paper I) have $L_{2-10\ \rm keV}/L_{\rm Edd}$ smaller than $L_{\rm X,crit}/L_{\rm Edd}$. In the right panel, we plot our data points with the fundamental plane of Yuan et al. (2009, black solid line, see Eq. (4)). The results are perfectly in line with the Yuan et al. (2009) prediction, in the sense that only the sources with $L_{2-10\ \rm keV}/L_{\rm Edd} < L_{\rm X,crit}/L_{\rm Edd}$, i.e., NGC 2787 and the three NGC 4278 observations with the lowest X-ray fluxes, follow their fundamental plane, with the rest of the sources being inconsistent with it. According to the authors work, this would mean that the sources in our sample are consistent with a RIAF-dominated X-ray emission process, with the exception of NGC 2787 and the three NGC 4278 observations with the lowest fluxes, where a jet is probably dominating the X-ray emission.

In Fig. 7, we show our LINER 1 data points plotted alongside the Plotkin et al. (2012) fundamental plane. At the 1σ level, our sample follow well the authors fundamental plane, with the only exception being NGC 2787 and the lowest NGC 4278 X-ray fluxes (note, however, that these exceptions disappear at the 2σ level). Plotkin et al. (2012) found that the coefficient of their fundamental plane are better explained with a jet model than the RIAF model (see above). Therefore, according to these authors

[8] Note here that Plotkin et al. (2012) choose their X-ray luminosities as their dependent variable, the traditional form of the fundamental plane that we choose to use here is easily recovered with a simple variable substitution, this gives $\log L_{\rm R} = 0.69 \log L_{\rm X} + 0.61 \log M_{\rm BH} + 4.19$.

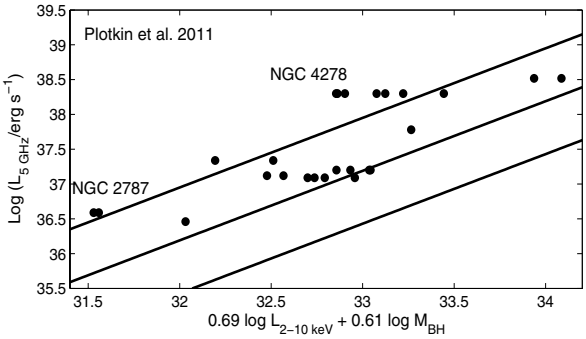

Fig. 7. Our sample of LINER 1s plotted with the fundamental plane of Plotkin et al. (2012). At the 1σ level, our sample is consistent with the authors fundamental plane, with the mild exception of the NGC 4278 observations with the lowest X-ray fluxes, and NGC 2787. See text for more details.

fundamental plane study, a jet synchrotron process appears to be the mechanism dominating the X-ray emission in our sample of LINER 1s.

The results we get looking at two different fundamental plane analysis came contradictory with one pointing toward a RIAF-dominated X-ray emission process and the other pointing toward a jet domination. Hence, using the fundamental plane by itself to distinguish X-ray processes is very challenging (as said by Plotkin et al. 2012), and clearly both a RIAF and a jet are at work with strong coupling between them. Nevertheless, it would be of great interest to study the fundamental plane of a big-enough, pure sample of AGN-powered LINERs, preferentially covering a large range in BH masses (e.g., three orders of magnitude), comparing the correlation coefficients with the ones expected from different radiative processes. Finally, before making any firm conclusion regarding the issue, one should look into all the different observational pieces together (e.g., Γ-Eddington-ratio, Paper I, and the $\alpha_{\rm ox}$-Eddington-ratio, this work, relations), then consider explaining them in a self-consistent manner.

6. Conclusion

We have studied the multiwavelength characteristics of the sample of LINERs showing a definite detection of broad Hα emission introduced in Paper I (LINER 1s, Ho et al. 1997b). Since the nuclear emission from LINERs could easily be contaminated from off-nuclear sources, high spatial resolution are required

at all wavelengths. Moreover, AGN-powered LINERs show a high degree of variability, especially in the UV and X-ray bands (Paper I; Maoz et al. 2005), hence simultaneous observations are crucial. Keeping these two points in mind, we collect from the literature VLA subarcsecond or VLBI milliarcsecond radio data and subarcsecond HST optical data. UV fluxes were derived from the OM instrument onboard *XMM-Newton*, and are simultaneous with the X-ray fluxes derived from the EPIC instrument.

We build the SED of six sources in our sample with *simultaneous UV and X-ray measurements*. We compare these SEDs, as well as their geometric mean SED, to the SED of a sample of radio-quiet and radio-loud quasars. At a given X-ray luminosity we find that, (1) our LINER 1s have radio luminosities comparable to the radio luminosity of radio-loud quasars, (2) the mean optical and UV luminosities are on average 5 to 10 times, respectively, smaller than in the quasar case, and (3) the X-ray spectral shape is similar to the spectral shape of radio-quiet quasars.

We calculate the UV to X-ray flux ratio, α_{ox}, of the six LINER 1s with simultaneous UV and X-ray fluxes and found $\alpha_{ox} = -1.17 \pm 0.02$ with a dispersion $\sigma = 0.01$, indicative of a weak UV excess relative to X-rays. We complement our results with α_{ox} values of a sample of AGN-powered LINERs (Maoz 2007; Pian et al. 2010). We find that α_{ox} is positively correlated to the Eddington ratio (considering negative α_{ox} values), in contrast to the relation established for luminous AGN (e.g., Lusso et al. 2010). This may be indicative of different emission processes producing the UV to X-ray spectral shape between AGN and LINERs.

Using high resolution radio fluxes at 5 GHz, we calculate the radio loudness parameter, $R_X = \nu L_\nu(5\ \mathrm{GHz})/L_{2-10\ \mathrm{keV}}$, for 11 of the 13 LINER 1s having radio core-emission detection. According to the Terashima & Wilson (2003) criterion, all of the 11 LINER 1s are considered radio-loud having $\log R_X > -4.5$. In fact 10 out of 11 LINER 1s have $\log R_X > -3.5$. We establish for the first time for LINER 1s, that this radio loudness parameter, R_X, is strongly anticorrelated to the Eddington ratio, confirming previous studies on LLAGN and luminous AGN sources. Moreover, we find a positive correlation between the radio luminosity and the X-ray luminosity which places AGN-powered LINERs, on a radio-power scale, right between low luminosity Seyferts and low luminosity radio galaxies.

Finally, we attempted to infer the X-ray emission mechanism in our sample of LINER 1s with the help of two different "fundamental planes of BH activity". The results were contradictory. The fundamental plane of Yuan et al. (2009) pointed toward a RIAF-dominated origin for the X-ray emission in our sample. On the other hand, Plotkin et al. (2012) fundamental plane indicates that our sample of LINER 1s may have a jet dominated X-ray emission.

Acknowledgements. This research has made use of observations made with the NASA/ESA *Hubble* Space Telescope, and obtained from the *Hubble* Legacy Archive, which is a collaboration between the Space Telescope Science Institute (STScI/NASA), the Space Telescope European Coordinating Facility (ST-ECF/ESA) and the Canadian Astronomy Data Centre (CADC/NRC/CSA). This research has made use of the NASA/IPAC Extragalactic Database (NED) which is operated by the Jet Propulsion Laboratory, California Institute of Technology, under contract with the National Aeronautics and Space Administration. This research has made use of the data obtained from the *Chandra Data Archive* and the *Chandra Source Catalog*, and software provided by the *Chandra X-ray Center* (CXC) in the application packages CIAO and Chips. This work is based on observations with *XMM-Newton*, an ESA science mission with instruments and contributions directly funded by ESA Member States and the USA (NASA). This research has made use of the SIMBAD database, operated at CDS, Strasbourg, France. G.Y. would like to thank Yadi Xu for enlightening discussions on ADAF models.

References

Alonso-Herrero, A., Rieke, M. J., Rieke, G. H., & Shields, J. C. 2000, ApJ, 530, 688
Anderson, J. M., & Ulvestad, J. S. 2005, ApJ, 627, 674
Anderson, J. M., Ulvestad, J. S., & Ho, L. C. 2004, ApJ, 603, 42
Avni, Y., & Tananbaum, H. 1982, ApJ, 262, L17
Awaki, H., Terashima, Y., Hayashida, K., & Sakano, M. 2001, PASJ, 53, 647
Balmaverde, B., Capetti, A., & Grandi, P. 2006, A&A, 451, 35
Barth, A. J., Ho, L. C., Filippenko, A. V., & Sargent, W. L. W. 1998, ApJ, 496, 133
Belsole, E., Worrall, D. M., & Hardcastle, M. J. 2006, MNRAS, 366, 339
Binder, B., Markowitz, A., & Rothschild, R. E. 2009, ApJ, 691, 431
Blandford, R. D. 1990, in Active Galactic Nuclei, ed. R. D. Blandford, H. Netzer, L. Woltjer, T. J.-L. Courvoisier, & M. Mayor, 161
Blandford, R. D., & Begelman, M. C. 1999, MNRAS, 303, L1
Blandford, R. D., & Konigl, A. 1979, ApJ, 232, 34
Brandt, W. N., Laor, A., & Wills, B. J. 2000, ApJ, 528, 637
Brinkmann, W., Laurent-Muehleisen, S. A., Voges, W., et al. 2000, A&A, 356, 445
Broderick, J. W., & Fender, R. P. 2011, MNRAS, 417, 184
Canosa, C. M., Worrall, D. M., Hardcastle, M. J., & Birkinshaw, M. 1999, MNRAS, 310, 30
Canvin, J. R., Laing, R. A., Bridle, A. H., & Cotton, W. D. 2005, MNRAS, 363, 1223
Capetti, A., & Balmaverde, B. 2006, A&A, 453, 27
Cardelli, J. A., Clayton, G. C., & Mathis, J. S. 1989, ApJ, 345, 245
Chiaberge, M., Capetti, A., & Macchetto, F. D. 2005, ApJ, 625, 716
Cotton, W. D., Feretti, L., Giovannini, G., Lara, L., & Venturi, T. 1999, ApJ, 519, 108
de Gasperin, F., Merloni, A., Sell, P., et al. 2011, MNRAS, 415, 2910
Di Matteo, T., Carilli, C. L., & Fabian, A. C. 2001, ApJ, 547, 731
Doi, A., Kameno, S., Kohno, K., Nakanishi, K., & Inoue, M. 2005, MNRAS, 363, 692
Done, C. 2002, Roy. Soc. London Phil. Trans. Ser. A, 360, 1967
Done, C., Gierliński, M., & Kubota, A. 2007, A&ARv, 15, 1
Dopita, M. A., & Sutherland, R. S. 1995, ApJ, 455, 468
Dudik, R. P., Satyapal, S., Gliozzi, M., & Sambruna, R. M. 2005, ApJ, 620, 113
Dunlop, J. S., McLure, R. J., Kukula, M. J., et al. 2003, MNRAS, 340, 1095
Elvis, M., Wilkes, B. J., McDowell, J. C., et al. 1994, ApJS, 95, 1
Eracleous, M., Hwang, J. A., & Flohic, H. M. L. G. 2010, ApJS, 187, 135
Falcke, H., & Markoff, S. 2000, A&A, 362, 113
Falcke, H., Nagar, N. M., Wilson, A. S., & Ulvestad, J. S. 2000, ApJ, 542, 197
Falcke, H., Körding, E., & Markoff, S. 2004, A&A, 414, 895
Fender, R., Corbel, S., Tzioumis, T., et al. 1999, ApJ, 519, L165
Filho, M. E., Barthel, P. D., & Ho, L. C. 2002, A&A, 385, 425
Filho, M. E., Barthel, P. D., & Ho, L. C. 2006, A&A, 451, 71
Flohic, H. M. L. G., Eracleous, M., Chartas, G., Shields, J. C., & Moran, E. C. 2006, ApJ, 647, 140
Fossati, G., Maraschi, L., Celotti, A., Comastri, A., & Ghisellini, G. 1998, MNRAS, 299, 433
Gambill, J. K., Sambruna, R. M., Chartas, G., et al. 2003, A&A, 401, 505
Gammie, C. F., Narayan, R., & Blandford, R. 1999, ApJ, 516, 177
González Delgado, R. M., Pérez, E., Cid Fernandes, R., & Schmitt, H. 2008, AJ, 135, 747
González-Martín, O., Masegosa, J., Márquez, I., Guerrero, M. A., & Dultzin-Hacyan, D. 2006, A&A, 460, 45
González-Martín, O., Masegosa, J., Márquez, I., Guainazzi, M., & Jiménez-Bailón, E. 2009, A&A, 506, 1107
Greene, J. E., & Ho, L. C. 2007, ApJ, 656, 84
Grupe, D., Komossa, S., Leighly, K. M., & Page, K. L. 2010, ApJS, 187, 64
Gu, M., & Cao, X. 2009, MNRAS, 399, 349
Gu, Q.-S., Huang, J.-S., Wilson, G., & Fazio, G. G. 2007, ApJ, 671, L105
Gültekin, K., Cackett, E. M., Miller, J. M., et al. 2009, ApJ, 706, 404
Hawley, J. F., & Balbus, S. A. 2002, ApJ, 573, 738
Healey, S. E., Romani, R. W., Taylor, G. B., et al. 2007, ApJS, 171, 61
Heckman, T. M. 1980, A&A, 87, 152
Heinz, S., & Sunyaev, R. A. 2003, MNRAS, 343, L59
Helmboldt, J. F., Taylor, G. B., Tremblay, S., et al. 2007, ApJ, 658, 203
Ho, L. C. 1999, ApJ, 516, 672
Ho, L. C. 2002, ApJ, 564, 120
Ho, L. C. 2008, ARA&A, 46, 475
Ho, L. C. 2009, ApJ, 699, 626
Ho, L. C., Filippenko, A. V., & Sargent, W. L. W. 1996, ApJ, 462, 183
Ho, L. C., Filippenko, A. V., & Sargent, W. L. W. 1997a, ApJS, 112, 315
Ho, L. C., Filippenko, A. V., Sargent, W. L. W., & Peng, C. Y. 1997b, ApJS, 112, 391
Ho, L. C., Feigelson, E. D., Townsley, L. K., et al. 2001, ApJ, 549, L51

Hummel, E. 1980, A&AS, 41, 151
Hummel, E., van der Hulst, J. M., & Dickey, J. M. 1984, A&A, 134, 207
Igumenshchev, I. V. 2004, Prog. Theor. Phys. Suppl., 155, 87
Igumenshchev, I. V., & Abramowicz, M. A. 2000, ApJS, 130, 463
Kelly, B. C., Bechtold, J., Siemiginowska, A., Aldcroft, T., & Sobolewska, M. 2007, ApJ, 657, 116
Kelly, B. C., Bechtold, J., Trump, J. R., Vestergaard, M., & Siemiginowska, A. 2008, ApJS, 176, 355
Kelly, B. C., Vestergaard, M., Fan, X., et al. 2010, ApJ, 719, 1315
Körding, E., Falcke, H., & Corbel, S. 2006, A&A, 456, 439
Kovalev, Y. Y., Kellermann, K. I., Lister, M. L., et al. 2005, AJ, 130, 2473
Krips, M., Eckart, A., Neri, R., et al. 2005, A&A, 442, 479
Krips, M., Eckart, A., Krichbaum, T. P., et al. 2007, A&A, 464, 553
Laing, R. A., Canvin, J. R., Cotton, W. D., & Bridle, A. H. 2006, MNRAS, 368, 48
Laor, A. 2000, ApJ, 543, L111
Li, Z.-Y., Wu, X.-B., & Wang, R. 2008, ApJ, 688, 826
Lusso, E., Comastri, A., Vignali, C., et al. 2010, A&A, 512, A34
Malkan, M. A., & Sargent, W. L. W. 1982, ApJ, 254, 22
Maoz, D. 2007, MNRAS, 377, 1696
Maoz, D., Filippenko, A. V., Ho, L. C., et al. 1996, ApJS, 107, 215
Maoz, D., Nagar, N. M., Falcke, H., & Wilson, A. S. 2005, ApJ, 625, 699
Markoff, S., Nowak, M., Young, A., et al. 2008, ApJ, 681, 905
Martel, A. R., Ford, H. C., Bradley, L. D., et al. 2004, AJ, 128, 2758
McKinney, J. C. 2006, MNRAS, 368, 1561
Meier, D. L. 1999, ApJ, 522, 753
Merloni, A., Heinz, S., & di Matteo, T. 2003, MNRAS, 345, 1057
Miller, B. P., Brandt, W. N., Schneider, D. P., et al. 2011, ApJ, 726, 20
Mushotzky, R. F., & Wandel, A. 1989, ApJ, 339, 674
Nagar, N. M., Falcke, H., Wilson, A. S., & Ho, L. C. 2000, ApJ, 542, 186
Nagar, N. M., Wilson, A. S., & Falcke, H. 2001, ApJ, 559, L87
Nagar, N. M., Falcke, H., Wilson, A. S., & Ulvestad, J. S. 2002, A&A, 392, 53
Nagar, N. M., Falcke, H., & Wilson, A. S. 2005, A&A, 435, 521
Nandra, K., George, I. M., Mushotzky, R. F., Turner, T. J., & Yaqoob, T. 1997, ApJ, 477, 602
Nandra, K., O'Neill, P. M., George, I. M., & Reeves, J. N. 2007, MNRAS, 382, 194
Narayan, R., & McClintock, J. E. 2008, New A Rev., 51, 733
Narayan, R., & Yi, I. 1994, ApJ, 428, L13
Narayan, R., & Yi, I. 1995a, ApJ, 444, 231
Narayan, R., & Yi, I. 1995b, ApJ, 452, 710
Nemmen, R. S., Storchi-Bergmann, T., Yuan, F., et al. 2006, ApJ, 643, 652
Nicholson, K. L., Reichert, G. A., Mason, K. O., et al. 1998, MNRAS, 300, 893
Pahre, M. A., Ashby, M. L. N., Fazio, G. G., & Willner, S. P. 2004, ApJS, 154, 235
Panessa, F., Barcons, X., Bassani, L., et al. 2007, A&A, 467, 519
Pian, E., Romano, P., Maoz, D., et al. 2010, MNRAS, 401, 677
Plotkin, R. M., Markoff, S., Kelly, B. C., Koerding, E., & Anderson, S. F. 2012, MNRAS, 419, 267
Porquet, D., Reeves, J. N., O'Brien, P., & Brinkmann, W. 2004, A&A, 422, 85
Pott, J.-U., Hartwich, M., Eckart, A., et al. 2004, A&A, 415, 27
Ptak, A., Yaqoob, T., Mushotzky, R., Serlemitsos, P., & Griffiths, R. 1998, ApJ, 501, L37
Ptak, A., Terashima, Y., Ho, L. C., & Quataert, E. 2004, ApJ, 606, 173
Quataert, E. 2001, in Probing the Physics of Active Galactic Nuclei, ed. B. M. Peterson, R. W. Pogge, & R. S. Polidan, ASP Conf. Ser., 224, 71
Quataert, E., Di Matteo, T., Narayan, R., & Ho, L. C. 1999, ApJ, 525, L89
Reeves, J. N., & Turner, M. J. L. 2000, MNRAS, 316, 234
Reeves, J. N., Turner, M. J. L., Ohashi, T., & Kii, T. 1997, MNRAS, 292, 468
Remillard, R. A., & McClintock, J. E. 2006, ARA&A, 44, 49
Shakura, N. I., & Sunyaev, R. A. 1973, A&A, 24, 337
Shang, Z., Brotherton, M. S., Wills, B. J., et al. 2011, ApJS, 196, 2
Shemmer, O., Brandt, W. N., Netzer, H., Maiolino, R., & Kaspi, S. 2008, ApJ, 682, 81
Shields, G. A. 1978, Nature, 272, 706
Sikora, M., Stawarz, Ł., & Lasota, J. 2007, ApJ, 658, 815
Sobolewska, M. A., Gierliński, M., & Siemiginowska, A. 2009, MNRAS, 394, 1640
Sobolewska, M. A., Siemiginowska, A., & Gierliński, M. 2011, MNRAS, 413, 2259
Sparke, L. S., van Moorsel, G., Schwarz, U. J., & Vogelaar, M. 2009, AJ, 137, 3976
Steffen, A. T., Strateva, I., Brandt, W. N., et al. 2006, AJ, 131, 2826
Strateva, I. V., Brandt, W. N., Schneider, D. P., Vanden Berk, D. G., & Vignali, C. 2005, AJ, 130, 387
Tananbaum, H., Avni, Y., Branduardi, G., et al. 1979, ApJ, 234, L9
Terashima, Y., & Wilson, A. S. 2003, ApJ, 583, 145
Terashima, Y., Ho, L. C., & Ptak, A. F. 2000, ApJ, 539, 161
Terlevich, R., & Melnick, J. 1985, MNRAS, 213, 841
Turner, T. J., George, I. M., Nandra, K., & Turcan, D. 1999, ApJ, 524, 667
Ulvestad, J. S., & Ho, L. C. 2001, ApJ, 562, L133
Vasudevan, R. V., & Fabian, A. C. 2009, MNRAS, 392, 1124
Vasudevan, R. V., Mushotzky, R. F., Winter, L. M., & Fabian, A. C. 2009, MNRAS, 399, 1553
Venturi, T., Giovannini, G., Feretti, L., Comoretto, G., & Wehrle, A. E. 1993, ApJ, 408, 81
Vignali, C., Brandt, W. N., & Schneider, D. P. 2003, AJ, 125, 433
Wang, R., Wu, X.-B., & Kong, M.-Z. 2006, ApJ, 645, 890
Willis, A. G., Strom, R. G., Bridle, A. H., & Fomalont, E. B. 1981, A&A, 95, 250
Wilson, A. S., & Colbert, E. J. M. 1995, ApJ, 438, 62
Worrall, D. M., & Wilkes, B. J. 1990, ApJ, 360, 396
Wu, Q., Yuan, F., & Cao, X. 2007, ApJ, 669, 96
Wu, Q., Cao, X., & Wang, D.-X. 2011, ApJ, 735, 50
Xu, Y.-D. 2011, ApJ, 739, 64
Younes, G., Porquet, D., Sabra, B., et al. 2010, A&A, 517, A33
Younes, G., Porquet, D., Sabra, B., & Reeves, J. N. 2011, A&A, 530, A149
Yu, Z., Yuan, F., & Ho, L. C. 2011, ApJ, 726, 87
Yuan, F. 2007, in The Central Engine of Active Galactic Nuclei, ed. L. C. Ho, & J.-W. Wang, ASP Conf. Ser., 373, 95
Yuan, F., & Cui, W. 2005, ApJ, 629, 408
Yuan, W., Brinkmann, W., Siebert, J., & Voges, W. 1998, A&A, 330, 108
Yuan, F., Markoff, S., & Falcke, H. 2002a, A&A, 383, 854
Yuan, F., Markoff, S., Falcke, H., & Biermann, P. L. 2002b, A&A, 391, 139
Yuan, F., Yu, Z., & Ho, L. C. 2009, ApJ, 703, 1034
Zamorani, G., Henry, J. P., Maccacaro, T., et al. 1981, ApJ, 245, 357
Zhang, W. M., Soria, R., Zhang, S. N., Swartz, D. A., & Liu, J. F. 2009, ApJ, 699, 281